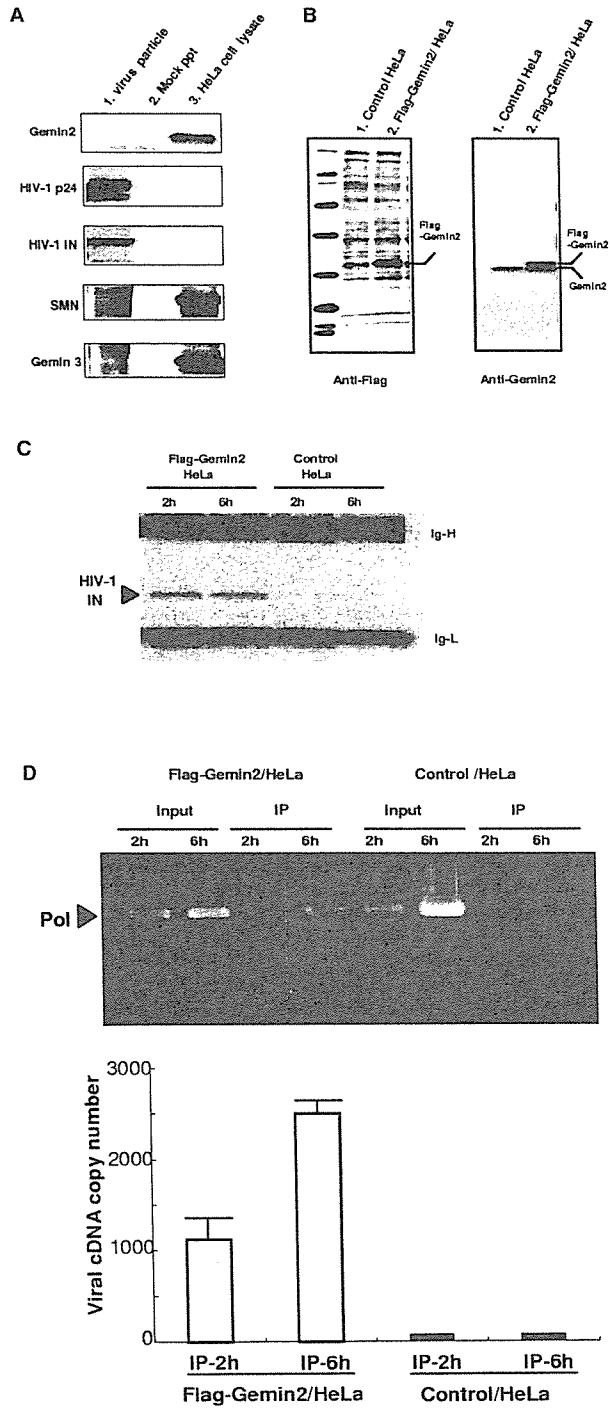

FIG. 2. Gemin2 interacts with the incoming HIV-1 genome complex. (A) Virus particles in the culture supernatant of 293T cells cotransfected with pNL43lucΔenv and pHCMVG were pelleted by ultracentrifugation (1 h at 315,000 × *g*) and subjected to Western blotting analysis using anti-Gemin2, anti-HIV-1 IN, or anti-p24 antibodies. Similarly prepared pellet fractions from mock-transfected cell supernatants (Mock ppt) and a HeLa whole-cell lysate were used as negative and positive controls, respectively. (B) HeLa cells were transduced with an empty vector (Control HeLa) or a FLAG-tagged Gemin2-expressing lentiviral vector (Flag-Gemin2/HeLa) and then subjected to Western blotting using an anti-FLAG antibody (left panel) or anti-Gemin2 antibody (right panel). (C) The transduced HeLa cells were infected with HIV-1 pseudotype virus. At 2 or 6 h postinfection, the cell lysates were immunoprecipitated with an anti-FLAG antibody and then subjected to Western blotting using an HIV-1 IN antibody. IgH, immunoglobulin heavy chain; IgL, immunoglobulin light chain. (D) Nucleic acids extracted from whole-cell lysates (input) or the IP obtained as described for panel C were subjected to PCR analysis of HIV-1 cDNAs. Amplified products (Pol) were separated in a 2% agarose gel and visualized by SYBR green staining (upper). The copy number of viral cDNA (R/gag) in each sample was estimated with real-time quantitative PCR (lower panel). Means ± standard errors (SE) from triplicate assays are shown.

transfected 293T cells (Fig. 3B, left panel). Furthermore, the progeny viruses released from the siGemin2-transfected 293T cell retained their infectivity (Fig. 3B, right panel). Thus, depletion of Gemin2 did not lead to any significant effect on proviral gene expression, virus release, or subsequent viral infectivity.

In contrast, HIV-1 infectivity was significantly reduced when the siGemin2 duplex was introduced into cells before viral infection (Fig. 3C). To exclude nonspecific or off-target effects (22) of the siGemin2 duplex originally tested here, we used four additional chemically modified synthetic siRNA duplexes (Stealth RNAi; Invitrogen) targeting different sequences within Gemin2 (Gemin2#372, Gemin2#373, Gemin2#374, and Gemin2#375) and an siGemin2 duplex carrying several nucleotide substitutions as a mismatch siGemin2 control (mm375). We observed significant reductions of HIV-1 infectivity that correlated well with the amount of specific reduction of Gemin2 with each type of siRNA treatment (Fig. 3C). In addition, we constructed an siRNA-resistant Gemin2 expression vector carrying silent point mutations in the target sequences of siGemin2#372. The siRNA-resistant Gemin2 continued to be expressed in the presence of siGemin2#372, but expression of the endogenous Gemin2 was greatly reduced (Fig. 3D lower). Under this condition, the siRNA-resistant Gemin2 rescued HIV-1 infectivity in siGemin2-treated cells (Fig. 3D upper). These results strongly suggest the functional role of Gemin2 through interaction with incoming HIV-1 genome complexes during the early steps of HIV-1 infection.

Functional role of Gemin2 in HIV-1 infection of primary nondividing cells. Next, we addressed the functional role of Gemin2 in HIV-1 infection of human primary MDMs, a model of major natural targets for HIV-1 infection in vivo. MDMs were isolated from three different healthy donors. Transfection of siGemin2 into MDMs markedly reduced HIV-1 infectivity to from 0.3% to 10% of the levels in the control MDMs (Fig. 4B, left panel). This remarkable effect of siGemin2 observed in MDMs could be partly explained by the fact that primary MDMs constitutively express a lower level of Gemin2 than the 293T and HeLa cell lines, which have been adapted in vitro (Fig. 4A). We confirmed that reduction of Gemin2 also suppressed spreading of replication-competent HIV-1 in MDMs to less than 10% of control level for at least 7 days (data not shown). As with the results obtained using 293T and HeLa cell lines, the siGemin2 duplex did not significantly affect HIV-1 expression when introduced into MDMs 24 h after infection (Fig. 4B, right panel).

Finally, we addressed the effect of depletion of Gemin2 on HIV-1 cDNA synthesis and subsequent integration using real-

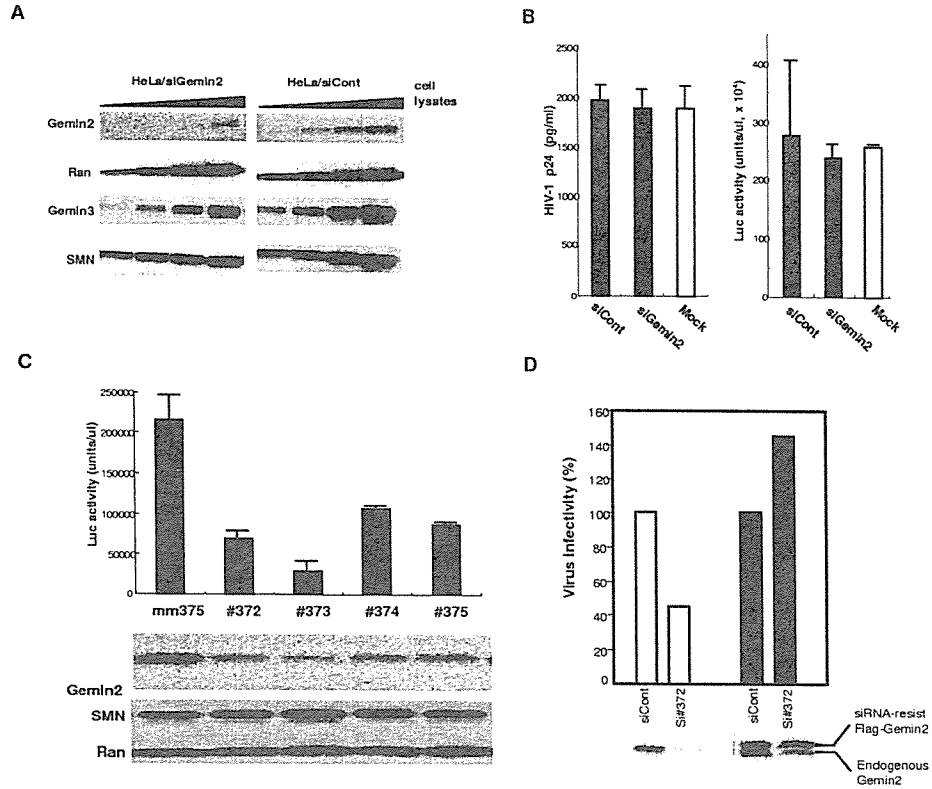

FIG. 3. Involvement of cellular Gemin2 in HIV-1 replication. (A) Total HeLa cell lysates prepared 48 h after transfection of siGemin2 (HeLa/siGemin2) or control siGFP (HeLa/siCont) were serially diluted twofold followed by Western blot analysis with antibodies against Gemin2, Ran, Gemin3, and SMN. (B) 293T cells were transfected with siGemin2 (black bar), siGFP (siCont; gray bar), or no siRNA (Mock; white bar), together with pNL-lucΔenv vector and pJD-1. The level of virus release from these 293T cells was determined by measuring HIV-1 p24 concentrations in the culture supernatant (left panel) 48 h posttransfection. These virus-containing supernatants were then incubated with HeLa cells. The cells were harvested 48 h postinfection and subjected to a luciferase assay (right panel). (C) HeLa cells were transfected with Stealth-siGemin2 (#372, #373, #374, or #375) or the control mismatch siGemin2 (mm375) 48 h before infection with HIV-1 pseudotype virus. The cells were harvested 48 h postinfection and subjected to a luciferase assay (upper panel) and Western blotting for Gemin2, SMN, and Ran (lower panel). (D) 293T cells were transfected with siRNA-resistant Flag-Gemin2 expression vector (black bars) or control empty vector (white bars) together with siGemin2#372 (si#372) or control siRNA (siCont) and then infected with HIV-1 pseudotype virus. The cells were harvested 24 h postinfection and subjected to a luciferase assay (upper) and Western blotting for endogenous Gemin2 and Flag-Gemin2 (lower). Virus infectivity is presented relative to the Luc activity in siCont-transfected cells, which was set to 100%.

time quantitative PCR analysis (20) in MDMs. Over time, the level of late reverse-transcription products (R/gag) was reduced in siGemin2-treated MDM (Fig. 4C) to ~5% of the level in the control siRNA-treated MDM at 48 h after HIV-1 infection (Fig. 4D). Of note, the amount of the early products of reverse transcription (R/U5) in the siGemin2-treated MDM was 30% to 40% of the level in the control siGFP-treated MDM (Fig. 4D). The region amplified for detection of the early reverse-transcription products (R/U5) is duplicated in the complete or nearly complete form of viral cDNA (late reverse transcription; R/gag) during the reverse-transcription step. Therefore, the marked reduction in the late reverse-transcription products by siGemin2 would be in part a consequence of the reduction in the duplication of the R/U5 region. The reduced amounts of the two-long terminal repeat (2-LTR) or integrated forms of cDNA observed in the siGemin2-treated MDMs could also be attributed to the inhibition of viral cDNA synthesis (2-LTR and integration; Fig. 4D). Thus, the dramatic reduction in the levels of late reverse-transcription products in the siGemin2-treated MDMs indicates that the abrogation of the reverse transcription of viral RNA might occur before or during the second template switch needed to complete the double-stranded viral cDNA copy, suggesting a role for Gemin2 during reverse transcription of the HIV-1 genome in vivo. We also confirmed that siGemin2 produced a similar effect on late RT products in HeLa cells. However, the inhibitory effect of siGemin2 on late RT products in HeLa cells was weaker than that in MDMs (data not shown). Therefore, possible roles of Gemin2 at other steps, including nuclear transport and integration of viral cDNA, cannot be ruled out.

Involvement of other constituents of the SMN complex. Under our experimental conditions, reduction of Gemin2 by siGemin2 was accompanied by slight decreases in SMN and Gemin3 levels (Fig. 3A and 4A). We addressed the critical point of whether Gemin2 acts on HIV-1 through the SMN complex or through another, unknown, complex by use of siRNAs targeting the other Gemin2-related proteins constituting the SMN complex. For each constituent of the complex—SMN (26), Gemin3 (6), Gemin4 (7), and Gemin6 (34)—we synthesized two or three chemically modified siRNA duplexes

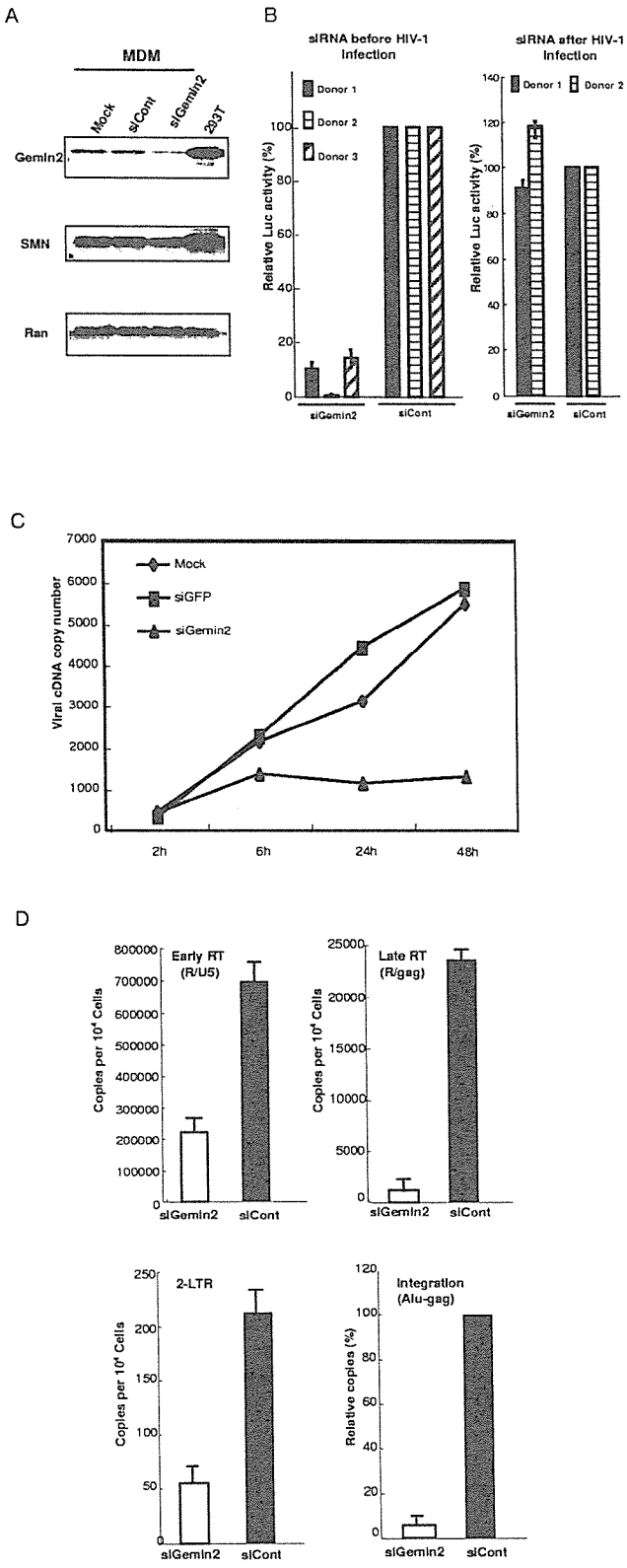

FIG. 4. Effect of siGemin2 on HIV-1 infection and cDNA synthesis in primary MDMs. (A) MDMs were transfected with siGemin2 or control siGFP (siCont) and subjected to Western blot analysis for Gemin2, SMN, and Ran. Mock, mock infected. (B) MDMs were transfected with each siRNA 24 h before (left panel) or after (right panel) infection with HIV-1 pseudotype virus. Cells were harvested and subjected to a luciferase assay 48 h (left panel) or 72 h (right panel) after infection. Relative Luc activity was calculated as a percentage of the control value in siCont-transfected cells. Each bar represents the value determined using MDMs prepared from different donors. Means ± SE from duplicate assays are shown. (C) MDMs were transfected with each siRNA 24 h before HIV-1 infection. Total DNA was extracted from siGemin2- or control siGFP-transfected MDMs at 2, 6, 24, and 48 h postinfection. Each sample was subjected to a quantitative analysis of viral cDNAs using real-time quantitative PCR with the primer pair M667-M661 (R/gag region) to measure the amount of complete or nearly complete viral cDNA (late RT). (D) Total DNA was extracted from MDMs transfected with siGemin2 or siGFP (siCont), infected with HIV-1 pseudotype virus for 48 h, and subjected to a quantitative analysis of viral cDNAs by use of real-time quantitative PCR with primer pair M667-AA55 (R/U5 region) for viral cDNA (Early-RT) or primer pair M667-M661 (R/gag region) for complete or nearly complete viral cDNA (Late-RT). We also monitored the formation of 2-LTR circular DNA by use of a primer pair that amplifies a sequence unique to the 2-LTR DNA junction and monitored the level of the integrated form of each viral cDNA by the Alu-PCR method using HIV-1-specific (M661) and Alu (Integration) primers. Results represent means ± SE.

targeting different sites within the coding sequence. Then we evaluated the effects of each siRNA on HIV-1 infection in HeLa cells (Fig. 5A). In parallel, the specific reduction in protein caused by each siRNA was also determined by examining protein expression profiles of the SMN constituents (Fig. 5B). Reduction of Gemin2 or SMN significantly blocked HIV-1 infection without showing apparent cell toxicity. However, siRNA duplexes against the SMN also significantly reduced Gemin2 levels (siSMN#271 and siSMN#272; Fig. 5B). In repeated experiments, the inhibitory effects of siSMNs on HIV-1 always correlated with the level of indirect reduction of Gemin2. Meanwhile, the reduction of Gemin3, Gemin4, and Gemin6 levels through their respective siRNA duplexes did not significantly affect HIV-1 infectivity, although siGemin3#432 and siGemin6#950 did inhibit HIV-1 infection by causing high cell toxicity. These results suggest that among the SMN constituents, Gemin2 is a critical constituent necessary to support HIV-1 infection. Thus, the effect of Gemin2 on HIV-1 infectivity might be independent of the other constituents of the SMN complex.

DISCUSSION

In this study, we have provided evidence that a novel host protein binds to HIV IN and modulates HIV-1 cDNA synthesis in vivo. We identified residues 137 to 238 of Gemin2 as binding to IN. In both the yeast two-hybrid system and a GST pull-down assay, the COOH-terminal domain of the IN was shown to be the minimum domain responsible for binding to Gemin2 (Fig. 1), although the central domain of the IN partly contributed to the binding. Gemin2 is a constituent of the SMN complex, along with other Gemin family proteins, including the putative DEAD box helicase dp103/Gemin3 (6), Gemin4 (7), Gemin5 (18), Gemin6 (34), and Gemin7 (2). Under our experimental conditions, treatment of cells with siGemin2 reduced the amount of Gemin2 protein and also resulted in slight decreases of SMN and Gemin3 levels (Fig. 3A and 4A).

Although the exact role of Gemin2 in the snRNP complex

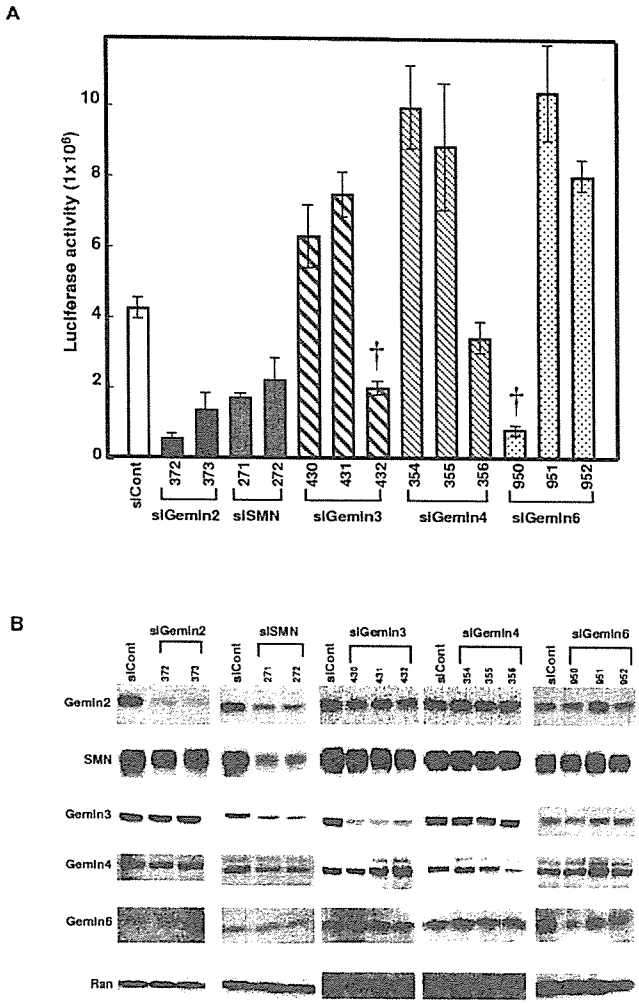

FIG. 5. Involvement of other constituents of the SMN complex. (A) HeLa cells were transfected with the Stealth siRNAs targeting Gemin2, Gemin3, Gemin4, Gemin6, or SMN 48 h before infection with HIV-1 pseudotype virus. The mismatch siGemin2 (mm375) was used as a negative control siRNA (siCont). The cells were harvested 48 h postinfection and subjected to a luciferase assay. Each bar represents the means ± SE. †, less than 20% of cells were viable 48 h after siRNA transfection. (B) Aliquots of the same cells harvested for the luciferase assay as described for panel A were subjected to Western blot analysis for Gemin2, SMN, Gemin3, Gemin4, Gemin6, and Ran.

remains to be determined, some reports suggest that it has a critical role in the assembly of the snRNP complex in the cytoplasm (3, 21, 30). More recently, the roles of the individual SMN constituents were addressed by using RNA interference (14). Feng et al. showed that a reduction of SMN leads to a decrease in snRNP assembly, the disappearance of bodies called Gems where SMN and Gemin2 are concentrated in the nucleus, and a drastic reduction in the amounts of several Gemins. Moreover, reduction of Gemin2 or Gemin6 levels strongly decreases the activity of the SMN complex. Therefore, we cannot exclude the possibility that a reduction of Gemin2 might also reduce SMN function under our experimental conditions. However, our data obtained using siRNAs targeting SMN, Gemin3, Gemin4, or Gemin6 suggest that Gemin2 is a critical constituent of the SMN complex for support of HIV-1 infection (Fig. 5). It seems likely that Gemin2 acts on the HIV-1 preintegration complex, either alone or with as-yet-unknown proteins other than the SMN constituents, although this point remains to be confirmed. In addition to the full-length Gemin2 (termed Gemin2-alpha), three splicing variants of Gemin2 (Gemin2-beta, -gamma, and -delta) have been identified (1). Gemin2-alpha has found to be ubiquitously expressed at high levels in the various normal tissues. In contrast, Gemin2-beta and -gamma are expressed at very low levels in these normal tissues (1). The Gemin2 residues that we identified as the region of Gemin2 that binds IN in the yeast two-hybrid system (residues 137 to 238, IBDG2) were shared by all splicing variants of Gemin2 except Gemin2-beta, in which residues 174 to 188 are deleted. It will be interesting to identify the contribution of other splicing variants of Gemin2 to HIV-1 infection.

The SMN complex has recently been reported to be generally used by infectious agents for RNP assembly (17). Golembe et al. demonstrated that herpesvirus saimiri uses the SMN complex to assemble Sm cores on its small RNAs (HSURs), just as occurs with host snRNPs. HSURs are the most abundant viral transcripts in latently infected, transformed T cells but are not essential for viral replication. Thus, the biological meaning of their complex formation remains to be determined. However, the authors suggest that infectious agents that engage the SMN complex may burden SMN-dependent pathways, possibly leading to a deleterious reduction in the availability of SMN complexes for essential host functions.

In the case of HIV-1 infection, we showed here that HIV-1 might require Gemin2 for efficient viral cDNA synthesis. Our results suggest that Gemin2, either alone or in concert with unidentified cellular proteins, supports HIV-1 infection, probably by supporting the reassembly of the reverse transcription complex to initiate and complete reverse transcription. Several cases of mutations in HIV-1 IN affecting reverse transcription have been described previously (11, 29, 37, 39, 42). It is, therefore, reasonable that a protein interacting with IN might play a role in reverse transcription and could also be involved in the subsequent nuclear transport and integration of viral cDNA. Since both reverse transcription and integration are essential steps for retrovirus infection, our findings will shed light on the functional role of IN during the reverse transcription of the retroviral genome and will also serve as the basis for a novel therapeutic approach to treat HIV-1 disease.

ACKNOWLEDGMENTS

We thank G. Dreyfuss for providing pTRE-FLAG-GEMIN2; I. S. Y. Chen for pNL43lucΔenv, pJD-1, and pHCMVG; and H. Miyoshi for pCSII-CMV-MCS. We also thank Y. Kawaguchi for technical advice on the yeast two-hybrid system and M. Kubo, S. Kaiga, N. Takahashi, M. Mogi, and S. Nishino for their technical assistance.

This work was supported by a Grant-in-Aid for Scientific Research on Priority Areas from the Ministry of Education, Culture, Sports, Science and Technology (MEXT) of Japan and a Health Sciences Research Grant from the Ministry of Health, Labor and Welfare of Japan (Research on HIV/AIDS13110201).

REFERENCES

1. **Aerbajinai, W., T. Ishihara, K. Arahata, and T. Tsukahara.** 2002. Increased expression level of the splicing variant of SIP1 in motor neuron diseases. Int. J. Biochem. Cell Biol. 34:699–707.

2. **Baccon, J., L. Pellizzoni, J. Rappsilber, M. Mann, and G. Dreyfuss.** 2002. Identification and characterization of Gemin7, a novel component of the survival of motor neuron complex. J. Biol. Chem. **277:**31957–31962.
3. **Buhler, D., V. Raker, R. Luhrmann, and U. Fischer.** 1999. Essential role for the tudor domain of SMN in spliceosomal U snRNP assembly: implications for spinal muscular atrophy. Hum. Mol. Genet. **8:**2351–2357.
4. **Bukrinsky, M. I., and O. K. Haffar.** 1997. HIV-1 nuclear import: in search of a leader. Front Biosci. **2:**d578–d587.
5. **Bukrinsky, M. I., N. Sharova, T. L. McDonald, T. Pushkarskaya, W. G. Tarpley, and M. Stevenson.** 1993. Association of integrase, matrix, and reverse transcriptase antigens of human immunodeficiency virus type 1 with viral nucleic acids following acute infection. Proc. Natl. Acad. Sci. USA **90:**6125–6129.
6. **Charroux, B., L. Pellizzoni, R. A. Perkinson, A. Shevchenko, M. Mann, and G. Dreyfuss.** 1999. Gemin3: a novel DEAD box protein that interacts with SMN, the spinal muscular atrophy gene product, and is a component of gems. J. Cell Biol. **147:**1181–1194.
7. **Charroux, B., L. Pellizzoni, R. A. Perkinson, J. Yong, A. Shevchenko, M. Mann, and G. Dreyfuss.** 2000. Gemin4. A novel component of the SMN complex that is found in both gems and nucleoli. J. Cell Biol. **148:**1177–1186.
8. **Cullen, B. R.** 2001. Journey to the center of the cell. Cell **105:**697–700.
9. **Elbashir, S. M., J. Harborth, W. Lendeckel, A. Yalcin, K. Weber, and T. Tuschl.** 2001. Duplexes of 21-nucleotide RNAs mediate RNA interference in cultured mammalian cells. Nature **411:**494–498.
10. **Engelman, A., F. D. Bushman, and R. Craigie.** 1993. Identification of discrete functional domains of HIV-1 integrase and their organization within an active multimeric complex. EMBO J. **12:**3269–3275.
11. **Engelman, A., G. Englund, J. M. Orenstein, M. A. Martin, and R. Craigie.** 1995. Multiple effects of mutations in human immunodeficiency virus type 1 integrase on viral replication. J. Virol. **69:**2729–2736.
12. **Fassati, A., and S. P. Goff.** 2001. Characterization of intracellular reverse transcription complexes of human immunodeficiency virus type 1. J. Virol. **75:**3626–3635.
13. **Fassati, A., and S. P. Goff.** 1999. Characterization of intracellular reverse transcription complexes of Moloney murine leukemia virus. J. Virol. **73:** 8919–8925.
14. **Feng, W., A. K. Gubitz, L. Wan, D. J. Battle, J. Dostie, T. J. Golembe, and G. Dreyfuss.** 2005. Gemins modulate the expression and activity of the SMN complex. Hum. Mol. Genet. **14:**1605–1611.
15. **Fischer, U., Q. Liu, and G. Dreyfuss.** 1997. The SMN-SIP1 complex has an essential role in spliceosomal snRNP biogenesis. Cell **90:**1023–1029.
16. **Goff, S. P.** 2001. Intracellular trafficking of retroviral genomes during the early phase of infection: viral exploitation of cellular pathways. J. Gene Med. **3:**517–528.
17. **Golembe, T. J., J. Yong, D. J. Battle, W. Feng, L. Wan, and G. Dreyfuss.** 2005. Lymphotropic *Herpesvirus saimiri* uses the SMN complex to assemble Sm cores on its small RNAs. Mol. Cell. Biol. **25:**602–611.
18. **Gubitz, A. K., Z. Mourelatos, L. Abel, J. Rappsilber, M. Mann, and G. Dreyfuss.** 2002. Gemin5, a novel WD repeat protein component of the SMN complex that binds Sm proteins. J. Biol. Chem. **277:**5631–5636.
19. **Hehl, E. A., P. Joshi, G. V. Kalpana, and V. R. Prasad.** 2004. Interaction between human immunodeficiency virus type 1 reverse transcriptase and integrase proteins. J. Virol. **78:**5056–5067.
20. **Ikeda, T., H. Nishitsuji, X. Zhou, N. Nara, T. Ohashi, M. Kannagi, and T. Masuda.** 2004. Evaluation of the functional involvement of human immunodeficiency virus type 1 integrase in nuclear import of viral cDNA during acute infection. J. Virol. **78:**11563–11573.
21. **Jablonka, S., M. Bandilla, S. Wiese, D. Buhler, B. Wirth, M. Sendtner, and U. Fischer.** 2001. Co-regulation of survival of motor neuron (SMN) protein and its interactor SIP1 during development and in spinal muscular atrophy. Hum. Mol. Genet. **10:**497–505.
22. **Jackson, A. L., S. R. Bartz, J. Schelter, S. V. Kobayashi, J. Burchard, M. Mao, B. Li, G. Cavet, and P. S. Linsley.** 2003. Expression profiling reveals off-target gene regulation by RNAi. Nat. Biotechnol. **21:**635–637.
23. **Kalpana, G. V., S. Marmon, W. Wang, G. R. Crabtree, and S. P. Goff.** 1994. Binding and stimulation of HIV-1 integrase by a human homolog of yeast transcription factor SNF5. Science **266:**2002–2006.
24. **Katz, R. A., and A. M. Skalka.** 1994. The retroviral enzymes. Annu. Rev. Biochem. **63:**133–173.
25. **Leavitt, A. D., G. Robles, N. Alesandro, and H. E. Varmus.** 1996. Human immunodeficiency virus type 1 integrase mutants retain in vitro integrase activity yet fail to integrate viral DNA efficiently during infection. J. Virol. **70:**721–728.
26. **Liu, Q., U. Fischer, F. Wang, and G. Dreyfuss.** 1997. The spinal muscular atrophy disease gene product, SMN, and its associated protein SIP1 are in a complex with spliceosomal snRNP proteins. Cell **90:**1013–1021.
27. **Maertens, G., P. Cherepanov, Z. Debyser, Y. Engelborghs, and A. Engelman.** 2004. Identification and characterization of a functional nuclear localization signal in the HIV-1 integrase interactor LEDGF/p75. J. Biol. Chem. **279:** 33421–33429.
28. **Maertens, G., P. Cherepanov, W. Pluymers, K. Busschots, E. De Clercq, Z. Debyser, and Y. Engelborghs.** 2003. LEDGF/p75 is essential for nuclear and chromosomal targeting of HIV-1 integrase in human cells. J. Biol. Chem. **278:**33528–33539.
29. **Masuda, T., V. Planelles, P. Krogstad, and I. S. Chen.** 1995. Genetic analysis of human immunodeficiency virus type 1 integrase and the U3 *att* site: unusual phenotype of mutants in the zinc finger-like domain. J. Virol. **69:** 6687–6696.
30. **Meister, G., D. Buhler, R. Pillai, F. Lottspeich, and U. Fischer.** 2001. A multiprotein complex mediates the ATP-dependent assembly of spliceosomal U snRNPs. Nat. Cell Biol. **3:**945–949.
31. **Miyoshi, H., U. Blomer, M. Takahashi, F. H. Gage, and I. M. Verma.** 1998. Development of a self-inactivating lentivirus vector. J. Virol. **72:**8150–8157.
32. **Nakamura, T., T. Masuda, T. Goto, K. Sano, M. Nakai, and S. Harada.** 1997. Lack of infectivity of HIV-1 integrase zinc finger-like domain mutant with morphologically normal maturation. Biochem. Biophys. Res. Commun. **239:** 715–722.
33. **Nymark-McMahon, M. H., N. S. Beliakova-Bethell, J. L. Darlix, S. F. Le Grice, and S. B. Sandmeyer.** 2002. Ty3 integrase is required for initiation of reverse transcription. J. Virol. **76:**2804–2816.
34. **Pellizzoni, L., J. Baccon, J. Rappsilber, M. Mann, and G. Dreyfuss.** 2002. Purification of native survival of motor neurons complexes and identification of Gemin6 as a novel component. J. Biol. Chem. **277:**7540–7545.
35. **Pellizzoni, L., J. Yong, and G. Dreyfuss.** 2002. Essential role for the SMN complex in the specificity of snRNP assembly. Science **298:**1775–1779.
36. **Sharp, P. A.** 2001. RNA interference—2001. Genes Dev. **15:**485–490.
37. **Tsurutani, N., M. Kubo, Y. Maeda, T. Ohashi, N. Yamamoto, M. Kannagi, and T. Masuda.** 2000. Identification of critical amino acid residues in human immunodeficiency virus type 1 IN required for efficient proviral DNA formation at steps prior to integration in dividing and nondividing cells. J. Virol. **74:**4795–4806.
38. **van Gent, D. C., C. Vink, A. A. Groeneger, and R. H. Plasterk.** 1993. Complementation between HIV integrase proteins mutated in different domains. EMBO J. **12:**3261–3267.
39. **Wu, X., H. Liu, H. Xiao, J. A. Conway, E. Hehl, G. V. Kalpana, V. Prasad, and J. C. Kappes.** 1999. Human immunodeficiency virus type 1 integrase protein promotes reverse transcription through specific interactions with the nucleoprotein reverse transcription complex. J. Virol. **73:**2126–2135.
40. **Yee, J. K., T. Friedmann, and J. C. Burns.** 1994. Generation of high-titer pseudotyped retroviral vectors with very broad host range. Methods Cell Biol. **43**(Pt. A):99–112.
41. **Yung, E., M. Sorin, A. Pal, E. Craig, A. Morozov, O. Delattre, J. Kappes, D. Ott, and G. V. Kalpana.** 2001. Inhibition of HIV-1 virion production by a transdominant mutant of integrase interactor 1. Nat. Med. **7:**920–926.
42. **Zhu, K., C. Dobard, and S. A. Chow.** 2004. Requirement for integrase during reverse transcription of human immunodeficiency virus type 1 and the effect of cysteine mutations of integrase on its interactions with reverse transcriptase. J. Virol. **78:**5045–5055.

JOURNAL OF VIROLOGY, Nov. 2004, p. 11563–11573 Vol. 78, No. 21
0022-538X/04/$08.00+0 DOI: 10.1128/JVI.78.21.11563–11573.2004

Evaluation of the Functional Involvement of Human Immunodeficiency Virus Type 1 Integrase in Nuclear Import of Viral cDNA during Acute Infection

Tamako Ikeda,[1,2] Hironori Nishitsuji,[1] Xin Zhou,[1] Nobuo Nara,[2] Takashi Ohashi,[1] Mari Kannagi,[1] and Takao Masuda[1]*

Departments of Immunotherapeutics[1] and Laboratory Medicine,[2] Graduate School of Medicine and Dentistry, Tokyo Medical and Dental University, Tokyo, Japan

Received 23 April 2004/Accepted 18 June 2004

Nuclear import of viral cDNA is a critical step for establishing the proviral state of human immunodeficiency virus type 1 (HIV-1). The contribution of HIV-1 integrase (IN) to the nuclear import of viral cDNA is controversial, partly due to a lack of identification of its bona fide nuclear localization signal. In this study, to address this putative function of HIV-1 IN, the effects of mutations at key residues for viral cDNA recognition (PYNP at positions 142 to 145, K156, K159, and K160) were evaluated in the context of viral replication. During acute infection, some mutations (N144Q, PYNP>KL, and KKK>AAA) severely reduced viral gene expression to less than 1% the wild-type (WT) level. None of the mutations affected the synthesis of viral cDNA. Meanwhile, the levels of integrated viral cDNA produced by N144Q, PYNP>KL, and KKK>AAA mutants were severely reduced to less than 1% the WT level. Quantitative PCR analysis of viral cDNA in nuclei and fluorescence in situ hybridization analysis showed that these mutations significantly reduced the level of viral cDNA accumulation in nuclei. Further analysis revealed that IN proteins carrying the N144Q, PYNP>KL, and KKK>AAA mutations showed severely reduced binding to viral cDNA but kept their karyophilic properties. Taken together, these results indicate that mutations that reduced the binding of IN to viral cDNA resulted in severe impairment of virus infectivity, most likely by affecting the nuclear import of viral cDNA that proceeds integration. These results suggest that HIV-1 IN may be one of the critical constituents for the efficient nuclear import of viral cDNA.

Human immunodeficiency virus type 1 (HIV-1) and other lentiviruses efficiently establish in nondividing as well as dividing cells a proviral state in which a double-stranded DNA copy of the viral genomic RNA (viral cDNA) is stably integrated into a chromosome of the host cell (5, 41, 64). This property distinguishes lentiviruses from certain other retroviruses that require mitosis with nuclear envelope breakdown prior to viral cDNA integration (42, 56).

The proviral state is established through several steps following binding to and entry into the target cell, including uncoating, reverse transcription, nuclear transport, and integration of the viral genome. These early events are mediated through the interactions of several viral proteins and host factors with the viral genome, often referred to as the reverse transcription complex and the preintegration complex (PIC) (reviewed in references 3, 13, and 29). The average diameter of HIV-1 PIC has been estimated to be ~56 nm (50), precluding its passive nuclear import through intact nuclear pore complexes on the nuclear envelope of host cells (reviewed in reference 13).

To facilitate the efficient nuclear import of HIV-1 cDNA, HIV-1 PIC may contain karyophiles with nuclear localization signal (NLS) sequences. Among the HIV-1 PIC constituents, matrix (MA) protein, viral protein R (Vpr), and integrase (IN) have been reported to have karyophilic properties (4, 14, 24, 26, 27, 32, 37, 54). However, several contradictory results have also been reported, arguing against this putative role for NLS sequences within the MA protein (25, 55) or Vpr (2) in the nuclear transport of viral cDNA. In addition, the *cis*-acting viral cDNA structure, the central DNA flap, generated during lentivirus-specific reverse transcription, has also been reported to play an important role in the nuclear import of the HIV-1 genome (68). However, recent studies have shown that the effect of the central DNA flap appears to be virus strain and host cell dependent (17, 44). Thus, key factors that facilitate the nuclear import of viral cDNA in the context of the viral replication cycle still remain to be determined.

Among the HIV-1 PIC constituents described above, IN is a logical and highly probable candidate for facilitating the efficient nuclear import of HIV-1 cDNA, since it has karyophilic properties (2, 14, 26, 43, 54, 60) and mediates the integration of viral cDNA into the host chromosome in nuclei. Previously, atypical bipartite NLS sequences within HIV-1 IN were reported to be recognized by the importin/karyopherin pathway (26). However, several studies showed that these NLS sequences did not mediate nuclear import but were instead required for reverse transcription of the viral genome or other steps in the viral replication cycle (53, 60). Recently, the Val and Arg residues at positions 165 and 166 (V165/R166) in HIV-1 IN were shown to be critical for its NLS function in mediating the nuclear import of viral cDNA (2). However, reassessments of V165/R166 functions have failed to confirm this conclusion (17, 43). Thus, despite many experimental at-

* Corresponding author. Mailing address: Department of Immunotherapeutics, Graduate School of Medicine and Dentistry, Tokyo Medical and Dental University, 1-5-45 Yushima, Bunkyo-ku, Tokyo 113-8519, Japan. Phone: 81 (3) 5803-5799. Fax: 81 (3) 5803-0235. E-mail: tmasu.impt@tmd.ac.jp.

TABLE 1. Mutations in HIV-1 IN

Mutant	Changes in:	
	Nucleotide[a]	Amino acid[b]
P142F	4654-CCC → *TTC*	P142 → F
Y143G	4657-TAC → *GGG*	Y143 → G
N144Q	4660-AAT → *CAA*	N144 → Q
P145F	4663-CCC → *TTC*	P145 → F
PYNP>KL	4654-CCC. . .4666-GTA → *AAGCTT*	PYNP (positions 142–145) → KL
K156A	4696-AAA → *GCA*	K156 → A
K159A	4705-AAG → *GCG*	K159 → A
K160A	4708-AAA → *GCA*	K160 → A
KKK>AAA	4696-AAA → *GCA*/4705-AAG → *GCG*/4708-AAA → *GCA*	KKK (positions 156, 159, and 160) → AAA

[a] Altered nucleotides are indicated by italic type. The nucleotide positions are numbered according to the NL43 sequence.
[b] Numbers are the amino acid residues of NL43 IN.

tempts, the contribution of HIV-1 IN to the nuclear import of viral cDNA remains controversial, partly due to a lack of identification of bona fide NLS sequences within IN. More recently, it was reported that the nuclear import of HIV-1 cDNA was mediated through the interaction of IN and importin 7, one of the host import factors for the nuclear import of ribosomal proteins and histone H1 (23). In addition, human lens epithelium-derived growth factor/transcription coactivator p75 (LEDGF/p75) was identified as an essential cellular factor for the chromosomal targeting of HIV-1 IN (47).

On the other hand, a detailed mechanism of retroviral integration was elucidated from in vitro studies with recombinant IN protein (reviewed in references 35 and 38). For the integration of viral cDNA, IN reacts with the attachment (*att*) site located at the U3 and U5 termini of the viral cDNA (12, 39, 48, 58, 61, 62). These studies of HIV-1 IN identified three functional domains: an N-terminal zinc binding domain (6–8), a central catalytic core domain (7, 11, 18, 57, 63), and a C-terminal nonspecific DNA binding domain (11, 19, 46). The central core domain contains the highly conserved D,D35E motif, which is directly involved in the catalytic activities of IN (7, 20, 30, 57). Tsurutani et al. previously reported that a single amino acid substitution of the Tyr residue at position 143 with Gly (Y143G) in HIV-1 IN significantly reduced the level of stably integrated proviral cDNA during acute infection of human primary cells (60). This reduction, concomitant with a reduction in the level of the two-long-terminal-repeat (2-LTR) circular form of viral cDNA, was evident in nondividing cells such as monocyte-derived macrophages (MDMs). Since circular forms of viral cDNA are produced in the nucleus, the Y143G mutation may affect the nuclear import of viral cDNA. The Y143 residue is located within the highly conserved core domain containing the D,D35E motif. The central core domain also contains several highly conserved residues critical for specific binding to viral cDNA (28, 33, 34, 40). These include Y143 (22, 45) and Lys residues at positions 156 (K156) (36, 67) and 159 (K159) (16, 36, 67). Thus, Y143 has been suggested to be one of the key residues for specific binding to viral cDNA.

In this study, we generated HIV-1 IN mutants carrying mutations at these key residues for viral cDNA recognition. Then, as an alternative approach to addressing the functional involvement of HIV-1 IN in the nuclear import of viral cDNA, the effects of these mutations were evaluated in the context of viral replication and the biochemical properties of the recombinant protein forms. Of note, mutations that reduced the binding of IN to viral cDNA resulted in the inefficient nuclear import of viral cDNA during acute infection. These results strongly suggest that HIV-1 IN may be a critical factor for the efficient transport of viral cDNA into nuclei.

MATERIALS AND METHODS

Construction of mutant DNA. DNA fragments for the mutagenesis of HIV-1 IN were derived from the HIV-1 pNL43lucΔenv vector (49), in which the *env* gene is defective, allowing the formation of pseudotypes, and the *nef* gene is replaced with the firefly luciferase gene. For the mutagenesis of IN mutants [P142F, Y143G, N144Q, P145F, PYNP>KL, K156A, K159A, K160A, and KKK (156/159/160) >AAA], a 1.6-kb fragment of the pNL43lucΔenv vector spanning the KpnI and SalI sites (nucleotides [nt] 4154 to 5785) was subcloned into pBluescript SKII(+) (Stratagene, La Jolla, Calif.) (pSKnK/S). To introduce mutations, all mutagenic primers were designed to span the NsiI and AflII sites (nt 4377 to 4743). PCR products amplified with each mutagenic primer pair (Table 1) and the pNL43lucΔenv vector as a template were digested with NsiI and AflII. The mutant fragments were ligated to NsiI-AflII-digested pSKnK/S. To generate some mutations with the backbone of the D116G mutation (D116G-ΔPYNP and D116G-KKK>AAA), mutagenic PCR was performed with each mutagenic primer pair and the pNL43lucΔenv vector carrying the D116G mutation (49) as a template. After confirmation of each mutation by DNA sequence analysis, KpnI-SalI fragments (nt 4154 to 5785) containing the mutations were ligated to the corresponding region in the 4.2-kbp SpeI-SalI fragment (nt 1507 to 5785). SpeI-SalI fragments containing the mutations were inserted back into the pNL43lucΔenv vector. The amplified region and cloning junctions were confirmed by DNA sequencing.

Cells. COS-7, 293T, HeLa, and RD cells were maintained in Dulbecco's modified Eagle medium (DMEM) supplemented with 10% fetal bovine serum (FBS). Human MDMs and peripheral blood lymphocytes (PBLs) were derived from HIV-1-seronegative healthy donors. Briefly, peripheral blood mononuclear cells were separated over a Ficoll-Hypaque gradient (Ficoll-Paque Plus; Amersham Pharmacia Biotech Inc., Tokyo, Japan) by centrifugation. Peripheral blood mononuclear cells were allowed to adhere to 150-mm plastic tissue culture dishes (Iwaki, Tokyo, Japan) by incubation in RPMI 1640 (Sigma Chemical Co., St. Louis, Mo.) containing 5% human AB serum (Sigma or Nippon Bio-Supply Center, Tokyo, Japan) for 2 h. Nonadherent cells (PBLs) were grown in RPMI 1640 medium containing 10% FBS and 2 ng of recombinant interleukin-2 (Shionogi, Osaka, Japan)/ml. Adherent cells were detached with cell dissociation solution (Sigma) and cultured in RPMI 1640 containing 5% human AB serum for 5 to 7 days. More than 98% of the cells that were shown to be positive for CD14, CCR5, HLA-DR, and mannose receptors were used as MDMs.

Virus preparation and infection. Pseudotype viruses were generated by cotransfection of COS-7 cells or 293T cells with the pNL43lucΔenv vector containing each IN mutation and an amphotropic Moloney murine leukemia virus (MuLV) envelope expression vector, pJD-1 (a kind gift from Irvin S. Y. Chen, University of California at Los Angeles), or a macrophage-tropic HIV-1 envelope vector, pJR-FL (a kind gift from Yoshio Koyanagi, Tohoku University), by using Lipofectamine (Invitrogen, Carlsbad, Calif.) or a calcium phosphate precipitation method. The culture supernatants (4 ml) of the transfected COS-7 cells

were harvested at 48 h posttransfection, filtered though 0.45-μm-pore-size filters, and used as the virus preparations. Each virus preparation was treated with DNase I (40 U/ml; Takara, Kyoto, Japan) in the presence of 10 mM $MgCl_2$ at 37°C for 1 h. To monitor residual contamination of the plasmid DNA, an aliquot of each virus preparation was incubated at 65°C for 1 h and used as a heat-inactivated control. To monitor the amount of virus in each preparation, the levels of HIV-1 p24 antigen were determined with an enzyme immunoassay system (RETRO-TEK; ZeptoMetrix Corp., Buffalo, N.Y.). To monitor viral gene expression from each plasmid vector, the luciferase activity in transfected COS-7 cells was also measured. At 48 h posttransfection, COS-7 cells were lysed with 1 ml of cell lysis buffer (Promega, Madison, Wis.), and then 1 μl of each cell lysate was subjected to a luciferase assay with Lumat LB 9507 (EG & G Berthold, Bad Wildbad, Germany). For virus infection, an aliquot (corresponding to ~20 ng of p24) of DNase I-treated virus was inoculated into RD cells (5×10^4), MDMs (5×10^5), or PBLs (1×10^6) in the presence of Polybrene (10 μg/ml). After incubation for 6 h at 37°C, the virus-containing medium was removed and replaced with fresh medium. At 4 days postinfection, the cells were harvested, washed twice with phosphate-buffered saline (PBS), and then lysed with 200 μl of cell lysis buffer. An aliquot (10 μl) of each lysate was subjected to the luciferase assay.

Western blot analysis. Viruses were concentrated by ultracentrifugation (1 h at 315,000 × *g* in a Beckman TLX-100 centrifuge with a TLA-100.4 rotor), and the pellets were resuspended in PBS. Viral proteins containing approximately 10 ng of p24 were subjected to sodium dodecyl sulfate (SDS)–12% polyacrylamide gel electrophoresis (PAGE). Following blotting of proteins onto a nitrocellulose membrane (ATTO, Tokyo, Japan), the membrane was incubated with antiserum from AIDS patients, anti-HIV-1 IN antibody (kindly provided by Duane Grandgenett, St. Louis University Health Sciences Center, Institute for Molecular Virology), or anti-HIV-1 p24 antibody (Chemicon International, Temecula, Calif.) followed by horseradish peroxidase-conjugated anti-human, anti-rabbit, or anti-mouse immunoglobulin. HIV-1 proteins were visualized by using an enhanced chemiluminescence detection system (Amersham Pharmacia Biotech, Tokyo, Japan).

Analysis of de novo-synthesized HIV-1 cDNA during acute infection. Total cells were harvested from each well at 1 or 2 days postinfection. After the cells were washed with PBS, nucleic acids were extracted as described previously (66). Briefly, the cells were disrupted in urea lysis buffer (4.7 M urea, 1.3% SDS, 0.23 M NaCl, 0.67 mM EDTA [pH 8.0]) and subjected to phenol-chloroform extraction and ethanol precipitation. The resulting DNA pellet was resuspended in 100 μl of distilled deionized water (ddw). An aliquot (5 μl) of each sample was subjected to PCR with a primer pair specific for the R/U5 region of HIV-1 (M667-AA55) or the R/gag region (M667-M661) (66). Detection of HIV-1 DNA sequences with each primer pair was performed by using PCR conditions of 30 cycles of 94°C for 1 min, 65°C for 2 min, and 72°C for 2 min. For DNA standards, 8 to 25,000 copies of linearized HIV-1 pNL43lucΔenv DNA were amplified in parallel. Quantitative analysis of the amplified products was performed by using a real-time Light Cycler detection system (Light Cycler Instrument; Roche, Mannheim, Germany). To normalize the amount of cellular DNA in the samples, a primer pair complementary to the first exon of the human β-globin gene was used. For the detection of human β-globin DNA, amplification was performed by using PCR conditions of 30 cycles of 94°C for 1 min, 55°C for 2 min, and 72°C for 2 min. A standard curve for human β-globin DNA was obtained by amplifying known amounts of cellular DNA from RD cells or MDMs in parallel. The 2-LTR circular DNA in nuclei was detected with specific primers as described previously (21). For detection of the integrated form of HIV-1 DNA, we used the Alu PCR method with an HIV-1-specific primer (M661) and an Alu-specific primer (5′-TCCCAGCTACTCGGGAGGCTGAGG-3′) (59). The cycling conditions were 94°C for 3 min, followed by 22 cycles of 94°C for 30 s, 66°C for 30 s, 70°C for 10 min, and then 72°C for 10 min. PCR products were purified and diluted 100- to 10,000-fold. The diluted samples were subjected to real-time PCR with the Light Cycler Instrument and an R/U5-specific primer pair (M667-AA55).

Confocal microscopic analysis of GFP-IN. HeLa cells (4×10^3) were seeded onto glass slides (Cel-Line; Erie Scientific Co, Portsmouth, N.H.) and transfected with a plasmid expressing green fluorescent protein (GFP) fused to full-length IN (60). At 24 h posttransfection, the cells were washed once with PBS and then fixed with 4% paraformaldehyde (Wako, Osaka, Japan) for 10 min. Confocal microscopy was performed with an Olympus BX50 fluorescence microscope (Olympus, Tokyo, Japan). Representative medial sections were mounted by using Adobe Photoshop software.

In vitro GST pull-down assay. DNA fragments encoding the entire HIV-1 IN were amplified by PCR with wild-type (WT) or each mutant plasmid DNA (pNL43lucΔenv) as a template. The primers used for the amplification of HIV-1 IN were as follows: GST-IN sense, 5′-GCGGATCCTTTTTAGATGGAATAG ATAAGGCCC-3′, and GST-IN end antisense, 5′-CCGGAATTCAATCCTCA TCCTG-3′; the sequences for BamHI or EcoRI recognition in each primer are underlined. Amplified products were digested with BamHI and EcoRI. Fragments with or without mutations were ligated to BamHI-EcoRI-digested vector pGEX-2T (Amersham Pharmacia Biotech). To express glutathione *S*-transferase (GST)–IN, *Escherichia coli* strain BL21(DE3) cells which had been transformed with pGEX-IN were grown in 16% Bacto Tryptone–10% yeast extract–5% NaCl–50 mg of carbenicillin/ml at 37°C to an optical density at 600 nm of 0.7. Expression was induced by the addition of 0.5 mM isopropyl-β-D-thiogalactoside (IPTG) for 17 h at 20°C. Cells were harvested by centrifugation and resuspended at a 1/10 volume of the original cell culture in high-salt buffer (1 M NaCl in PBS) containing 1 mM phenylmethylsulfonyl fluoride (PMSF), 1 mM dithiothreitol (DTT), and a proteinase inhibitor mixture (1 μg of pepstatin A/ml, 2 μg of aprotinin/ml, and 0.5 μg of leupeptin/ml). Cells were lysed by sonication (Sonifier; Branson, Danbury, Conn.) followed by centrifugation at 19,000 × *g* for 30 min. The supernatant fraction of the cell lysate was incubated with glutathione-Sepharose 4B beads (Amersham Pharmacia Biotech) at 4°C overnight. The recombinant protein-bound beads were washed extensively with a wash buffer (1 M NaCl–1% Tween 20 in PBS) and then eluted with elution buffer (50 mM Tris-HCl [pH 8.0], 10 mM reduced glutathione) containing the proteinase inhibitor mixture at 25°C for 2 h. The eluted fraction containing the recombinant GST-IN protein was dialyzed against IN storage buffer {20 mM HEPES [pH 7.5], 0.1 mM EDTA, 0.3 M NaCl, 20% glycerol, 10 mM 3-[(3-cholamidopropyl)-dimethylammonio]-1-propanesulfonate [CHAPS], 10 mM DTT}. The purity of each recombinant GST-IN protein was confirmed by PAGE, and the protein concentrations were determined by the Bradford method.

The HIV-1 cDNA for the pull-down assay was prepared from crude PIC fractions (31). Briefly, MOLT-4/IIIB cells were cocultured with MOLT-4 cells for 6 h. Cells were harvested and permeabilized with 0.025% digitonin in buffer K (20 mM HEPES [pH 7.4], 150 mM KCl, 5 mM $MgCl_2$) followed by sequential centrifugations at 1,000 × *g* for 10 min and 12,000 × *g* for 20 min. The supernatants were used as crude PIC fractions. Viral cDNA was extracted from the crude PIC fractions by the urea lysis method as described above. The amount of viral cDNA was determined by real-time PCR with R/U5- and R/gag-specific primers. Viral cDNA (~10^5 copies) was incubated with each GST-IN protein (200 nM) immobilized on glutathione-Sepharose beads in binding buffer (20 mM HEPES [pH 7.3], 7.5 mM $MnCl_2$, 1 mM DTT, 1 mM PMSF, 10% polyethylene glycol) for 15 min at 4°C. The beads were washed five times with a wash buffer (1.0% Triton X-100 in PBS) and eluted with elution buffer. Viral cDNA bound to each GST-IN protein was extracted by phenol-chloroform treatment followed by ethanol precipitation with a carrier (Ethachinmate; Wako/Nippon Gene Co., Tokyo, Japan). The resulting DNA pellet was suspended in ddw. The amount of viral cDNA in each preparation was determined by real-time PCR with the M667-AA55 (R/U5-specific) or the M667-M661 (R/gag-specific) primer pair. The background level due to nonspecific binding of the input viral cDNA to GST protein and glutathione-Sepharose beads was determined by carrying out the same experiment with GST only in parallel. After subtraction of the background level (~5,000 copies per total input of ~10^5 copies), the relative copy number (R/gag) for each mutant as a percentage of that for the WT was calculated.

Isolation of DNA from the nuclear fraction. RD or 293T cells (5×10^6) were infected with each pseudotype virus and harvested at 24 h postinfection. For the isolation of nuclei, cells were resuspended in buffer A (10 mM HEPES [pH 7.3], 1.5 mM $MgCl_2$, 10 mM KCl, 0.5 mM DTT, 0.2% NP-40), homogenized by 20 strokes with an all-glass Dounce homogenizer (Kontes, Vineland, N.J.), and centrifuged at 500 × *g* for 5 min at 4°C. The pellet of the cell lysate was washed twice with Nuclei EZ Lysis Buffer and then with Nuclei Storage Buffer (Sigma). Nuclei were collected by centrifugation at 25,000 × *g* for 20 min at 4°C. DNA samples from each nuclear fraction were subjected to real-time PCR with the M667-AA55 (R/U5-specific) or the M667-M661 (R/gag-specific) primer pair as described above.

FISH analysis with HIV-1-specific PNA probes. For fluorescence in situ hybridization (FISH) analysis with HIV-1-specific peptide nucleic acid (PNA) probes (51), glass slides (Cel-Line) were coated with 3-aminopropyl triethoxysilane (silane; Aldrich). HeLa cells (4×10^3) seeded on the silane-coated slides were cultured overnight. Pseudotype viruses were prepared by cotransfection of 293T cells with the pNL43lucΔenv vector together with the MuLV envelope expression vector (pJD-1). After treatment with DNase I (40 μg/ml; Worthington), each virus (70 ng of p24) was inoculated into HeLa cells and cultured at 37°C for 6 h. The cells were washed with PBS and resuspended in fresh medium (DMEM plus 10% FBS). After 18 h, the cells were harvested and fixed with 4% paraformaldehyde for 30 min, and the slides were treated with proteinase K (2 ng/ml) for 8 min at room temperature and then with RNase A (10 ng/ml) for 10

min at room temperature. Endogenous biotin reactivity was blocked by the addition of 0.3% H_2O_2 in methanol. The slides were dehydrated in absolute ethanol.

Fluorescein isothiocyanate (FITC)-conjugated PNA probes were synthesized by Fasmac Co. (Kanagawa, Japan). The structure of the antisense probe was as follows: FITC-5′-GCACATTGTACTGATA-3′; this sequence corresponded to nt 2878 to 2994 of the *pol* region of pNL43 (1). The hybridization solution (Dako, Carpinteria, Calif.) containing the FITC-conjugated PNA probes was mounted on the slides, boiled for 5 min at 93°C, and then incubated for 17 h at 57°C. The slides were washed twice with a stringent wash solution (Dako) at 45°C for 20 min. After being washed with Tris-buffered saline containing 0.1% Tween 20 (TBST), the slides were reacted with 63 pg of a horseradish peroxidase (HRP)-conjugated anti-FITC antibody (Vector, Burlingame, Calif.)/ml for 30 min at 37°C. The slides were washed with TBST and reacted with biotinyl-tyramide (Dako) for 15 min at room temperature. After being washed with TBST, the slides were reacted with HRP-conjugated streptavidin (Dako). The slides were washed with TBST and reacted with biotinyl-tyramide for 15 min. Finally, the slides were reacted with 250 ng of Alexa 488-conjugated streptavidin/ml to detect the hybridized probes. Nuclei were stained with 125 ng of 4′,6′-diamidino-2-phenylindole (DAPI; Wako)/ml. The signals were observed with a confocal microscope (Olympus BX50). We counted the signal dots inside the nuclei of 20 to 50 cells from three independent hybridizations. Representative medial sections were mounted by using Adobe Photoshop software.

RESULTS

Construction of HIV-1 IN mutants. We introduced single amino acid substitutions or deletions at highly conserved Pro-Tyr-Asn-Pro residues (PYNP) spanning positions 142 to 145 or the three Lys residues at positions 156, 159, and 160 (K156, K159, and K160) in HIV-1 IN (Table 1), which are regions that contain several key residues critical for viral cDNA recognition (16, 22, 36, 45, 67). The mutations (Table 1) included a Pro-to-Phe substitution at position 142 (P142F), a Tyr-to-Gly substitution at position 143 (Y143G), an Asn-to-Gln substitution at position 144 (N144Q), a Pro-to-Phe substitution at position 145 (P145F), deletion of the PYNP motif at positions 142 to 145 by replacement with Lys-Leu (PYNP>KL), and Ala substitution(s) at each or all of the Lys residues at positions 156, 159, and 160 (K156A, K159A, K160A, and KKK>AAA). Due to the lack of identification of bona fide NLS sequences within IN, the effects of these mutations, which were expected to be defective at binding to viral cDNA, were evaluated in the context of viral replication, as an alternative approach to addressing the functional involvement of HIV-1 IN in the nuclear import of viral cDNA.

Infectivity of each HIV-1 IN mutant. A single-round infection system that uses an HIV-1 (pNL43lucΔBg) pseudotype virus is useful for estimating reverse transcription and integration efficiency in vivo by monitoring the levels of de novo-synthesized viral cDNA and luciferase activity produced in infected cells (48, 49, 60). Therefore, we examined the effect of each mutation on early events in viral replication by using the single-round infection system. Briefly, pseudotype viruses were generated by cotransfection of COS-7 cells with pNL43lucΔenv containing the WT or each IN mutation together with an expression vector for the amphotropic Moloney MuLV envelope (pJD-1) or the macrophage-tropic HIV-1 envelope (pJR-FL). At 48 h posttransfection, all mutants had comparable levels of p24 in culture supernatants harvested from transfected COS-7 cells (Fig. 1A) and comparable levels of luciferase activity in lysates of transfected COS-7 cells (data not shown). Thus, none of the mutations had a significant effect on transfected proviral gene expression or virus release.

In order to verify the Gag-Pol polyprotein processing in mutant virus particles, we performed Western blotting analyses of viral proteins contained in the virus particles with serum from an AIDS patient or antibodies to HIV-1 IN or p24. No apparent differences between the parental (WT) and mutant viruses were observed in the profiles (Fig. 1B and C). These

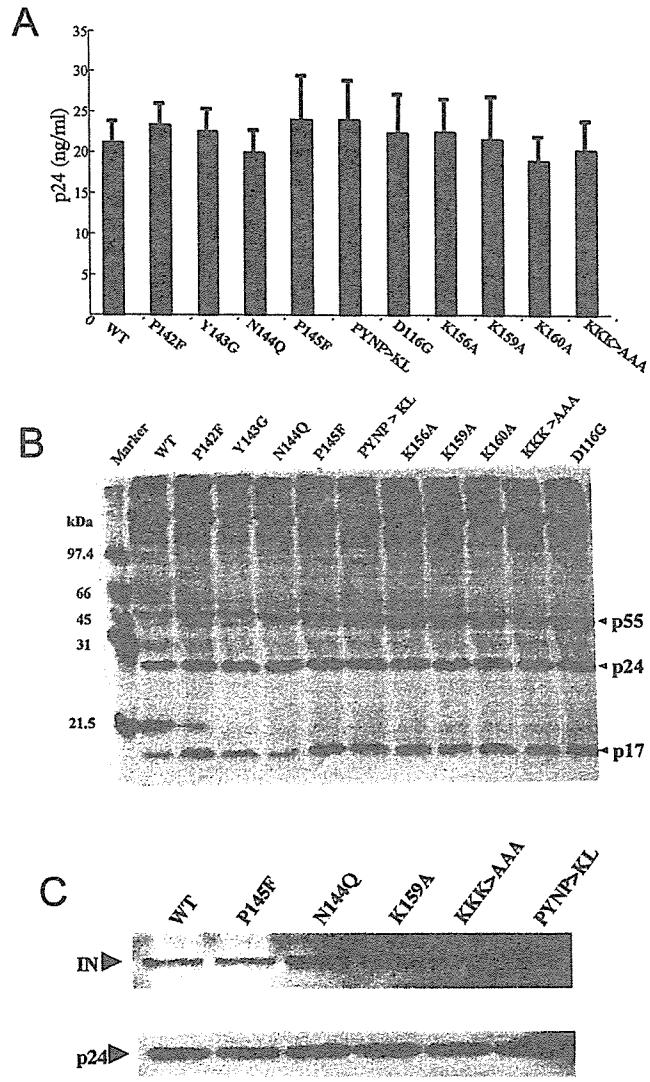

FIG. 1. Gene expression of each mutant proviral DNA after transfection of COS-7 cells and viral protein profiles. Pseudotype viruses were generated by cotransfection of COS-7 cells with the pNL43lucΔenv vector containing mutations in IN and an amphotropic Molony MuLV envelope expression vector (pJD-1) by using Lipofectamine. Culture supernatants (5 ml) of the transfected COS-7 cells were harvested at 48 h posttransfection. (A) p24 levels in culture supernatants were determined with the RETRO-TEK enzyme immunoassay system. (B and C) Virus particles in culture supernatants (5 ml) of COS-7 cells were precipitated at 48 h posttransfection by ultracentrifugation (1 h at 315,000 × *g* in a Beckman TLX-100 centrifuge). Viral proteins were separated by SDS–12% PAGE. After blotting of proteins onto a nitrocellulose membrane, the membrane was reacted with serum from an AIDS patient (B) or anti-HIV-1 IN or anti-p24 antibody (C) and then incubated with horseradish peroxidase-conjugated anti-human, anti-rabbit, or anti-mouse immunoglobulin. Viral proteins were visualized by using the enhanced chemiluminescence detection system. The positions of the major viral proteins are indicated.

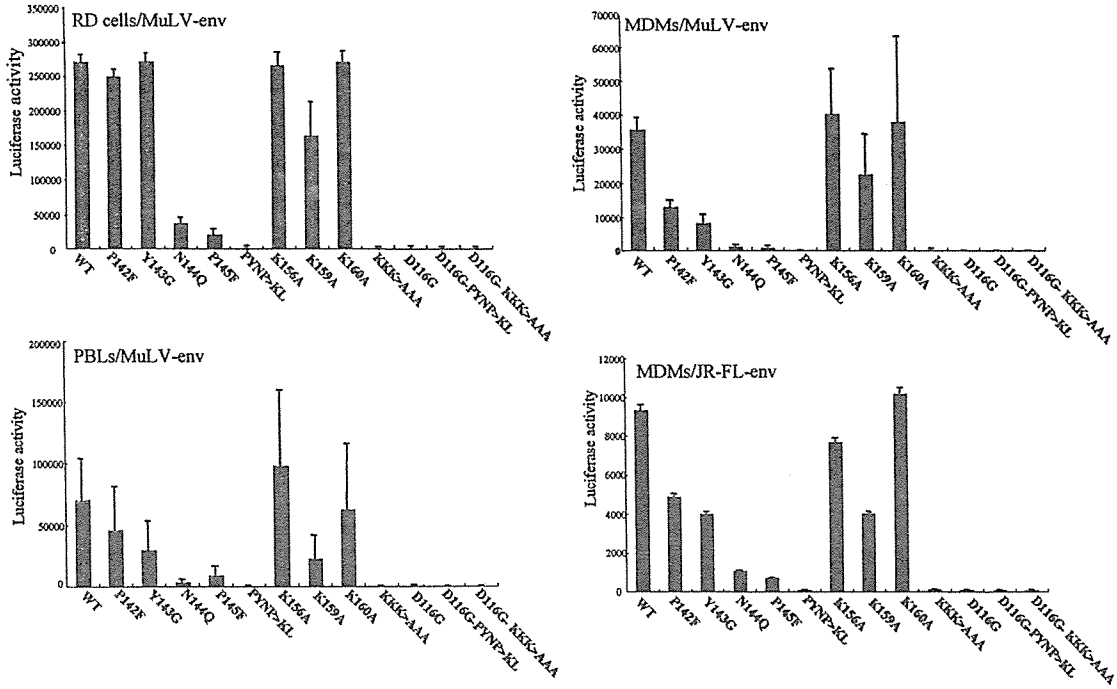

FIG. 2. Effects of HIV-1 IN mutations on viral infectivity. Viruses were prepared by cotransfection of COS-7 cells with the pNL43lucΔenv vector containing either WT IN or mutant IN together with an amphotropic Moloney MuLV envelope expression vector (pJD-1) or a macrophage-tropic HIV-1 envelope vector (pJR-FL) by using Lipofectamine. At 48 h posttransfection, culture supernatants of the transfected COS-7 cells were harvested. DNase I-treated supernatants were inoculated into 10^5 RD cells, PBLs, and MDMs. At 4 days postinfection, the cells were washed with PBS and lysed with 200 μl of cell lysis buffer. Ten microliters of each cell lysate was subjected to the luciferase assay. Mean values from five independent experiments are shown with the error bars.

results showed that none of the mutations significantly affected the late stage of viral replication from proviral gene expression to virus particle release, Gag-Pol polyprotein processing, and IN incorporation into the virus particles.

For virus infection, a DNase I-treated preparation of each pseudotype virus was inoculated into RD cells, MDMs, or PBLs. To examine the level of viral gene expression for each HIV-1 IN mutant, the luciferase activity expressed in infected cells was measured at 4 days postinfection. In this experiment, an IN mutant carrying a single amino acid substitution at one of the catalytic sites (D116G) was used as a control for integration-defective mutants (49). We repeated this experiment more than 10 times with independently prepared viruses (Fig. 2). In RD cells, the PYNP>KL mutation or the KKK>AAA mutation severely reduced the luciferase activity to less than 1% the WT level, which was similar to the level seen with the catalytic site mutation (D116G). The severe effects induced by these mutations were also observed after acute infection of human primary PBLs and MDMs. A significant reduction in the level of luciferase gene expression was also detected with some mutants with single amino acid substitutions in the PYNP motif (residues 142 to 145) or at K156, K159, and K160. The levels of luciferase activity produced by N144Q and P145F were significantly lower in RD cells, PBLs, and MDMs and ranged from 3 to 15% the WT level. As reported in a previous study (60), the effect of the Y143G mutation in the PYNP motif was more evident in primary cells (PBLs and MDMs) than in RD cells. Like Y143G, P142F (a single amino acid substitution in the same PYNP motif) produced lower levels of luciferase activity (24 to 65% the WT level) in PBLs and MDMs but produced a high level (90 to 100% the WT level) in RD cells. Thus, the integrity of the PYNP motif is more rigidly required for virus infection in primary cells (PBLs and MDMs) than in an in vitro-adapted cell line (RD cells). In addition, K159A produced a modest but consistent reduction in luciferase activity (42 to 60% the WT level), while other point mutations in the K residues (K156A and K160A) produced levels of luciferase activity comparable to that produced by the WT in all cell types. Since the KKK>AAA mutation produced a severe reduction in luciferase activity (<1% the WT level), the three Lys residues may function in a compensatory manner. Furthermore, these severe defects were efficiently complemented when WT IN was supplied in *trans* (data not shown), thus excluding possible effects of the mutations on *cis*-acting functions of the central polypurine tract (10, 68). Taken together, these results suggested important roles of PYNP at residues 142 to 145 and of K at residues 156, 159, and 160 in *trans*-acting functions of IN in the early events of the HIV-1 replication cycle.

Quantitative analysis of viral cDNA after infection with HIV-1 IN mutants. Next, we assessed the ability of each mutant to synthesize viral cDNA and to form integrated proviral cDNA following infection of RD cells (Fig. 3). At 24 h after infection with DNase I-treated virus, total DNA was harvested from infected RD cells, and an aliquot of each DNA sample was subjected to real-time quantitative PCR analysis. First, we monitored the formation of various species of viral cDNAs by using the M667-AA55 (R/U5-specific) primer pair for early

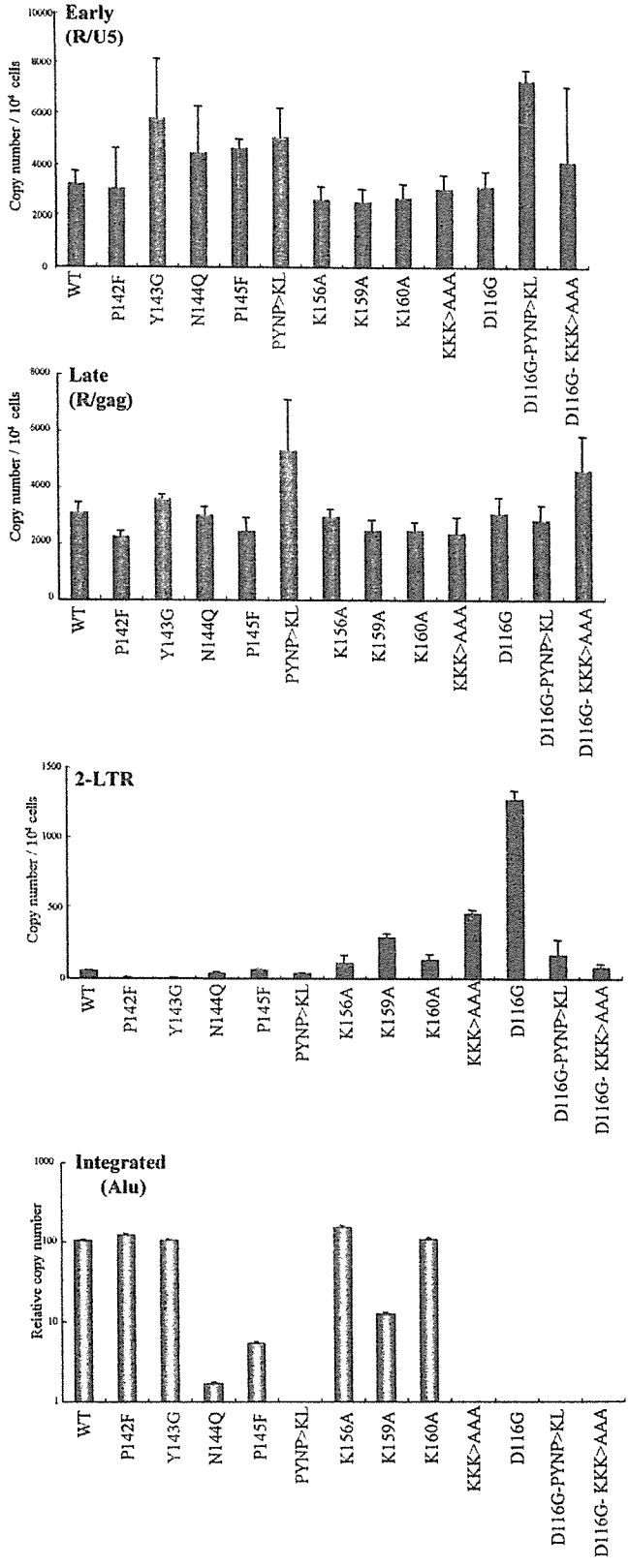

FIG. 3. Analysis of viral cDNA synthesis and proviral DNA formation. Each virus was prepared by cotransfection of COS-7 cells with pNL43lucΔenv (WT or mutant IN) together with pJD-1. DNase I-treated supernatants were inoculated into RD cells as described in the legend to Fig. 2. Viruses treated at 65°C for 1 h prior to inoculation were used as a heat-inactivated control. At 1 day postinfection, the entire cell culture was harvested, and total DNAs were extracted from infected RD cells. Each DNA sample was subjected to real-time quantitative PCR analysis with primer pairs specific for early (R/U5), late (R/gag), 2-LTR circular (2-LTR), or integrated (Alu) forms of viral cDNAs. The estimated copy number of each viral cDNA (R/U5, R/gag, 2-LTR, and Alu) per 10^5 cell equivalents is shown. For estimation of integrated viral cDNA (Alu), each DNA sample was subjected to PCR with the Alu- and R/gag-specific primer pair. Serial dilutions of each PCR product (Alu and R/gag) were subjected to real-time quantitative PCR with the R/U5-specific primer pair. Values were calculated as the copy number (R/U5) of each mutant relative to that of the WT, taken as 100%. Mean values from five independent experiments are shown with the error bars.

viral cDNA (early) and the M667-M661 (R/gag-specific) primer pair for complete or nearly complete viral cDNA (late). Relative to the WT, all PYNP motif mutants (P142F, Y143G, N144Q, P145F, and PYNP>KL) as well as K mutants K156A, K159A, K160A, and KKK>AAA produced comparable levels of early (R/U5) and complete or nearly complete (R/gag) forms of viral cDNA products. These results showed that none of these mutations affected reverse transcription.

Since all of the mutations in the PYNP and K residues produced comparable levels of complete or nearly complete viral cDNA products (R/gag), we next examined the fate of each de novo-synthesized viral cDNA in RD cells. To this end, we monitored the formation of 2-LTR circular DNA (Fig. 3, 2-LTR) by using a primer pair which amplified a sequence unique to the 2-LTR DNA junction (21). We also monitored the level of the integrated form of each viral cDNA by the Alu PCR method (59) with an HIV-1-specific primer (M661) and an Alu-specific primer (Fig. 3, Integrated). Products of 2-LTR DNA have been used as markers for its presence in the nucleus, since the enzymes responsible for its formation are thought to be located within the nucleus. In addition, 2-LTR DNA is formed in the absence of the catalytic function of IN (60). PCR amplification of this structure therefore confirms the specific inhibition of integration. An HIV-1 IN catalytic site mutant (D116G) (49) was used as a control for integration-defective mutants. As in a previous study (60), we clearly detected an amplified fragment corresponding to the 2-LTR circular junction in DNA samples from RD cells infected with integration-defective mutant D116G. Meanwhile, the P142F, Y143G, K156A, and K160A mutants as well as the WT produced much lower levels of 2-LTR DNA (2 to 9% the level produced by D116G), suggesting successful integration of viral cDNA. These conclusions were consistent with the level of expression of each viral gene (luciferase activity) shown in Fig. 2 and were further confirmed by Alu PCR analysis (Fig. 3, Integrated). On the other hand, the N144Q, P145F, PYNP>KL, K159A, and KKK>AAA mutants produced 2-LTR DNA at various levels—3, 5, 3, 23, and 36% the level produced by D116G, respectively (Fig. 3, 2-LTR). Of note, the levels of 2-LTR produced by these mutants were not always correlated with the reduction in luciferase activity (Fig. 2) or the integration level (Fig. 3, Integrated). In particular, the PYNP>KL mutant showed significant reductions in the level of luciferase activity (<2% the WT level) and integration (below the detection level). These phenotypes of PYNP>KL were almost iden-

tical to those of D116G. However, the level of 2-LTR DNA produced by PYNP>KL was only ~3% the level produced by D116G. Similar discrepancies were also noted for the N144Q and KKK>AAA mutants. In addition, a similar reduction in the level of 2-LTR DNA caused by the PYNP>KL and KKK>AAA mutations was reproduced on the backbone of the D116G mutation (Fig. 3, D116G-PYNP>KL and D116G-KKK>AAA). Taken together, these data suggested that the reduced levels of integration and subsequent gene expression seen with PYNP>KL, N144Q, and KKK>AAA might have been partly due to a reduction in the nuclear import of viral cDNA that precedes integration.

Interaction of IN protein with viral cDNA. Some of the IN mutants (PYNP>KL, N144Q, and KKK>AAA) showed a severe integration-defective phenotype, partly due to a failure to transport the viral cDNA into the nucleus. These mutants were generated by introducing mutations at critical residues in IN for viral cDNA recognition (16, 22, 36, 45, 67). Therefore, we next examined the binding of these IN proteins to viral cDNA. Viral cDNA (~10^5 copies) extracted from cells acutely infected with HIV-1 was incubated with 200 nM each GST-IN protein (WT, N144Q, PYNP>KL, or KKK>AAA) immobilized on glutathione-Sepharose beads. After extensive washing, the viral cDNA bound to each GST-IN protein was extracted. The amount of viral cDNA in each preparation was determined by real-time PCR with a primer pair specific for late forms (R/gag) of viral cDNA products (Fig. 4A). The levels of viral cDNA pulled down by GST-IN protein containing N144Q, PYNP>KL, and KKK>AAA were 2.1, 3.8, and 11.7% the WT level, respectively (Fig. 4A). Whether these in vitro data can be extrapolated to biological relevance in vivo still remains to be determined, but the PYNP>KL, N144Q, and KKK>AAA mutations reduced the binding of IN to viral cDNA at least in our in vitro assay.

Nuclear localization of IN fused to GFP. Tsurutani et al. previously reported that GFP-IN fusions efficiently localized to the nuclei of transiently transfected cells (60). We next examined the effects of the N144Q, PYNP>KL, K159A, and KKK>AAA mutations on the karyophilic properties of IN. Briefly, HeLa cells were transfected with GFP-IN expression vectors and subjected to analysis by confocal microscopy at 24 h posttransfection. In agreement with the previous report (60), GFP-IN accumulated predominantly in the nucleus [Fig. 4B, GFP-IN (WT)], while the GFP control protein was uniformly scattered throughout both the cytoplasm and the nucleus (Fig. 4B, GFP). Under the same conditions, IN mutants (N144Q, PYNP>KL, and KKK>AAA) were efficiently localized to the nucleus (Fig. 4B), suggesting that none of these mutations affected the karyophilic properties of IN.

Localization of HIV-1 cDNA during acute infection. The experimental data described above indicated that the loss of binding to viral cDNA seen with the IN mutations resulted in the decreased accumulation of viral cDNA in the nuclei. To confirm these observations more directly, we first determined the levels of viral cDNA in nuclear fractions isolated from acutely infected cells. 293T cells were infected with a DNase I-treated preparation of each pseudotype virus. At 24 h postinfection, nuclei were isolated from the cells. The levels of viral cDNA in the nuclei were determined by real-time PCR with a primer pair specific for R/U5 to monitor the total viral cDNA

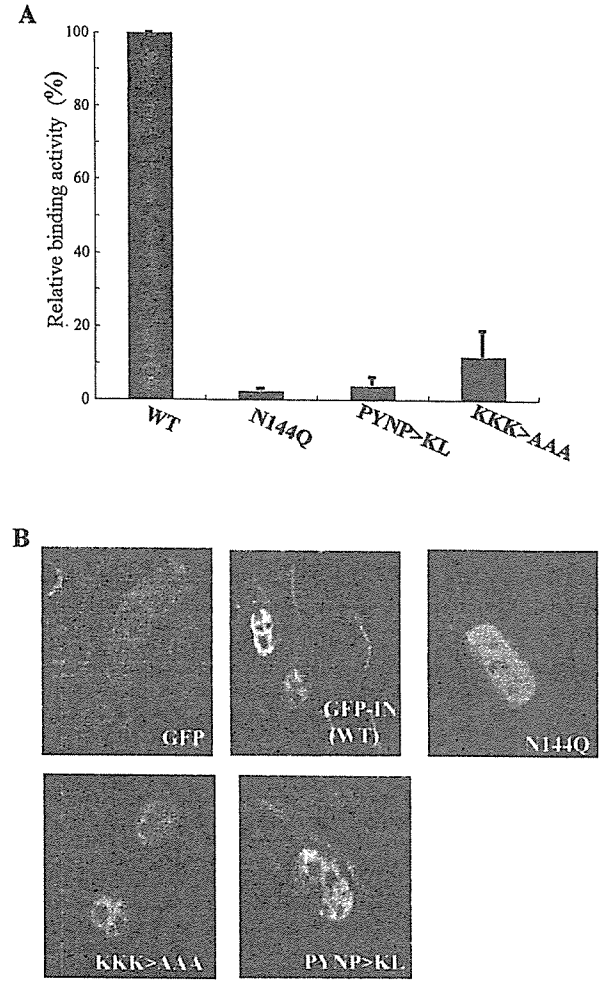

FIG. 4. Properties of HIV-1 IN mutant proteins. (A) Interactions of IN proteins with HIV-1 cDNA. Viral cDNA (~10^5 copies) extracted from a crude PIC fraction (see Materials and Methods) was incubated with 200 nM each GST-IN protein (WT, N144Q, PYNP>KL, and KKK>AAA) immobilized on glutathione-Sepharose beads in binding buffer. The beads were washed five times with a wash buffer (1.0% Triton X-100 in PBS) and eluted with elution buffer. Viral cDNA bound to each GST-IN protein was extracted by phenol-chloroform treatment followed by ethanol precipitation. The resulting DNA pellet was resuspended in ddw. The amount of viral cDNA in each preparation was measured by a real-time PCR system with a primer pair specific for the late product (R/gag) of viral cDNA. The values shown are the copy number (R/gag) of each mutant relative to that of the WT, taken as 100%. Mean values from three independent experiments are shown with the error bars. (B) Confocal microscopic analysis of GFP-IN. HeLa cells were transfected with a plasmid expressing GFP only, GFP fused to full-length IN (WT), or IN carrying the PYNP>KL, N144Q, or KKK>AAA mutation by using Lipofectamine. At 24 h posttransfection, the cells were fixed and examined with a confocal fluorescence microscope.

in the nuclei. The levels of viral cDNA in the nuclei after infection with the N144Q, PYNP>KL, KKK>AAA, and D116G IN mutants were 50.3, 38.9, 43.6, and 90.3% the WT level, respectively (Fig. 5A). These data indicated that the nuclear import of viral cDNA was significantly decreased by the N144Q, PYNP>KL, and KKK>AAA mutations ($P < 0.005$) but not by the D116G mutation ($P = 0.14$). Similar significant reductions in the levels of viral cDNA in the nuclei seen with

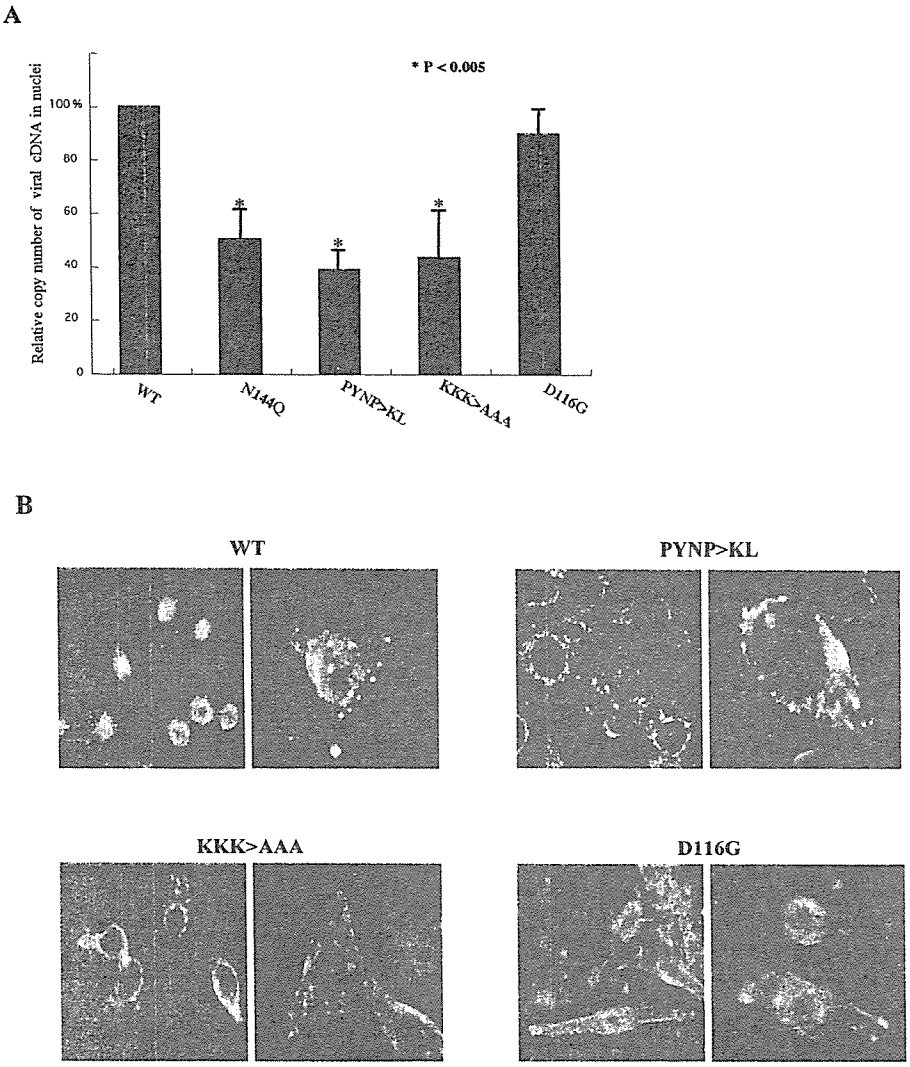

FIG. 5. Localization of HIV-1 cDNA after infection with each mutant. (A) Quantification of HIV-1 cDNA in the nuclear fraction. 293T cells were infected with each virus (WT, N144Q, PYNP>KL, KKK>AAA, or D116G). At 24 h postinfection, nuclei were isolated from the infected cells as described in Materials and Methods. A DNA sample from each nuclear fraction was subjected to real-time quantitative PCR with the M667-AA55 (R/U5-specific) or the M661-M667 (R/gag-specific) primer pair. The values shown are the copy number (R/U5) of each mutant per 10^4 nuclei relative to that of the WT, taken as 100%. Means and standard deviations from three independent experiments are shown ($n = 5$). (B) HeLa cells (4×10^3) were seeded on silane-coated glass slides. Cells were infected with each IN mutant (PYNP>KL, KKK>AAA, or D116G) or with the WT (~70 ng of p24). At 6 h postinfection, the cells were fixed with 4% paraformaldehyde and subjected to FISH analysis with an FITC-labeled HIV-1-specific PNA probe corresponding to nt 2878 to 2994 of the *pol* region of pNL43 (1). The signals were observed with a confocal microscope. Representative medial sections were mounted by using Adobe Photoshop software. The representative cells in each slide are shown with lower (left) and higher (right) magnification scales.

the N144Q, PYNP>KL, and KKK>AAA mutations were reproduced when a primer pair specific for R/gag was used (data not shown).

Finally, we analyzed the subcellular localization of de novo-synthesized viral cDNA during acute infection by FISH. Briefly, HeLa cells were infected with a DNase I-treated pseudotype virus of each IN mutant, incubated for 6 or 24 h, fixed, and subjected to FISH with an FITC-tagged HIV-1-specific PNA probe. Hybridized probe signals were detected by using a CAS system (Dako) with Alexa 488 and were visualized with an Olympus confocal laser scanning microscope (Fig. 5B). The majority (~78%) of the signals produced by the WT or the D116G mutant were in the nuclei at 6 h postinfection. In contrast, under the same conditions, markedly fewer signals were detected in the nuclei after infection with the PYNP>KL and KKK>AAA mutants. These signals in the cytoplasm tended to be weakened at 24 h postinfection (data not shown), suggesting that PYNP>KL and KKK>AAA might reduce the nuclear accumulation of viral cDNA partly because these mutant PICs were more susceptible to degradation. Although we cannot rule out the partial contribution of the effect of these mutations on the stability of viral cDNA and/or the PIC, these results indicated that the nuclear transport that precedes the integration of viral cDNA was significantly reduced by muta-

tions that reduced the binding affinity of HIV-1 IN for viral cDNA.

DISCUSSION

In this study, we generated HIV-1 IN mutants carrying mutations at key residues for viral cDNA recognition (16, 22, 36, 45, 67) and evaluated the effects of these mutations in the context of viral replication and the biochemical properties of the protein forms. Our major finding was that mutations reducing the interaction of IN with viral cDNA caused a severe impairment of integration, most likely by affecting the efficient nuclear import of viral cDNA.

Despite many experimental data indicating the karyophilic properties of HIV-1 IN (2, 14, 26, 43, 54, 60), the contribution of IN to the nuclear import of viral cDNA remains controversial. This situation may be partly due to a lack of identification of bona fide NLS sequences within IN. We also generated IN mutants by amino acid substitution of the V165/R166 residues that have been reported to be critical residues for an NLS within HIV-1 IN (2). However, our mutant (V165R/R166L) showed a complete lack of viral infectivity due to a failure to complete viral cDNA synthesis. Moreover, this IN mutant protein was unstable when expressed in the form of a GFP-IN fusion (data not shown). Thus, we cannot evaluate the importance of the V165/R166 residues in the karyophilic properties of IN or in the nuclear transport of viral cDNA in the context of viral replication. Recently, reassessments of these V165/R166 functions by use of IN mutants with Ala substitutions at the V165/R166 residues were reported by two different laboratories (17, 43). Both of these reports failed to confirm the NLS functions. Instead, V165A/R166A mutants were shown to be pleiotropic IN mutants primarily defective in integration. These conclusions are partly consistent with our data.

More recently, Devroe et al. reported that HIV-1 IN is unable to access the nucleus when expressed in the form of a large fusion with GFP and pyruvate kinase, suggesting that IN may lack a transferable NLS (15). Alternatively, they showed that cytoplasmic IN is highly unstable and prone to degradation and that the karyophilic properties can be attributed to an interaction with a cellular component. Interestingly, one of the nuclear factors, LEDGF/p75, has been identified as being essential for the karyophilic properties of HIV-1 IN, although the functional role of cytoplasmic LEDGF/p75 in the nuclear import of IN remains to be determined (47).

Meanwhile, genetic analyses of HIV-1 IN (9, 21, 49, 52, 60, 65) have suggested putative roles for IN at steps prior to integration, such as uncoating, reverse transcription, and nuclear import of viral cDNA. It was previously reported that a single amino acid substitution of the Tyr residue at position 143 with Gly (Y143G) in HIV-1 IN significantly reduced the level of stably integrated proviral DNA during acute infection of human primary cells. This reduction, concomitant with a reduction in the level of the 2-LTR circular form of viral cDNA, was evident in primary PBLs and MDMs (60); these data suggest that Y143 is a critical residue for efficient proviral DNA formation at steps prior to integration, most likely the nuclear import of viral cDNA. Y143 is located in the central catalytic domain of IN and is suggested to be one of the critical residues for specific binding to viral cDNA (22, 45). Thus, we reasoned that we could address the functional involvement of HIV-1 IN in the nuclear import of viral cDNA by using IN mutants that show reduced binding to viral cDNA.

Structural and biochemical analyses of HIV-1 IN identified three functional domains (reviewed in references 35 and 38): an N-terminal zinc binding domain, a central catalytic core domain, and a C-terminal nonspecific DNA binding domain. The central core domain contains the highly conserved D,D35E motif, which is directly involved in the catalytic activities of IN. The central core domain also contains several highly conserved residues critical for specific binding to viral cDNA. These include Y143, K156, K159, and K160 (16, 22, 36, 45, 67). In this study, we generated IN mutants by introducing single or triple amino acid substitutions or deletions of the highly conserved Pro-Tyr-Asn-Pro residues (PYNP) spanning positions 142 to 145 or three Lys residues (K156, K159, and K160) of HIV-1 IN (Table 1). We found that some of the IN mutant proteins carrying single amino acid substitutions in or deletions of the PYNP motif at positions 142 to 145 (N144Q and PYNP>KL) or a triple amino acid substitution for the three conserved Lys residues at positions 156, 159, and 160 (KKK>AAA) showed a severe reduction in binding to viral cDNA but retained their efficient karyophilic properties (Fig. 4B). However, whether these in vitro data can be extrapolated to biological relevance in vivo still remains to be determined. In the context of viral replication, HIV-1 carrying these IN mutations showed viral gene expression severely reduced to less than 1% the WT level, similar to the effects of a catalytic site mutation of IN (D116G) (Fig. 2). These defects were efficiently complemented by supplying WT IN in *trans* (data not shown), excluding the possible effects of these mutations on *cis*-acting functions of the central polypurine tract (10, 68).

Quantitative analysis of viral cDNA after infection with these HIV-1 IN mutants indicated that these mutations did not affect the de novo synthesis of viral cDNA products (Fig. 3, R/U5 and R/gag) but did severely reduce integration (Fig. 3, Integrated). Of note, the level of 2-LTR DNA, a surrogate marker for nuclear import, produced by the PYNP>KL mutant was only ~3% that produced by the catalytic site mutant D116G. A similar reduction in the level of 2-LTR DNA was also noted for the N144Q and KKK>AAA mutants, even on the backbone of the D116G mutation (Fig. 3, 2-LTR), suggesting that inhibition of the binding of IN to viral cDNA may affect the nuclear import of viral cDNA that precedes integration. This conclusion was further confirmed by more direct methods quantifying viral cDNA in isolated nuclei and FISH analyses of acutely infected cells (Fig. 5). However, although the signals of viral cDNA for the KKK>AAA and D116G-PYNP>KL mutants were evident at 6 h postinfection (Fig. 5B), they tended to be weakened at 24 h postinfection (data not shown), suggesting that PYNP>KL and KKK>AAA may reduce the nuclear accumulation of viral cDNA partly because these mutant PICs are more susceptible to degradation. Thus, an alternate explanation for the results is that if IN does not bind to viral cDNA, then the PIC falls apart and is nonfunctional. Although we cannot rule out the partial contribution of the effect of these mutations on the stability of viral cDNA and/or the PIC, our results indicate that the nuclear transport that precedes the integration of viral cDNA was significantly

reduced by mutations that reduced the binding affinity of HIV-1 IN for viral cDNA.

In summary, our findings indicate that IN mutants that were defective in viral cDNA recognition lost viral infectivity, thereby partly affecting the nuclear import of viral cDNA that precedes integration during acute infection with HIV-1. Taken together, these results suggest that HIV-1 IN may be one of the critical constituents for the efficient nuclear import of viral cDNA.

ACKNOWLEDGMENTS

We thank I. S. Y. Chen and Y. Koyanagi for providing plasmids, D. P. Grandgenett for providing anti-IN antibodies, and R. Yoshinari and S. Nishino for technical assistance.

This work was supported by a grant-in-aid for scientific research on priority areas from the Ministry of Education, Culture, Sports, Science, and Technology of Japan and a grant from the Ministry of Health, Labor and Welfare, Japan (Research on prevention of HIV replication and mutation 16150301).

REFERENCES

1. **Adachi, A., H. E. Gendelman, S. Koenig, T. Folks, R. Willey, A. Rabson, and M. A. Martin.** 1986. Production of acquired immunodeficiency syndrome-associated retrovirus in human and nonhuman cells transfected with an infectious molecular clone. J. Virol. **59:**284–291.
2. **Bouyac-Bertoia, M., J. D. Dvorin, R. A. Fouchier, Y. Jenkins, B. E. Meyer, L. I. Wu, M. Emerman, and M. H. Malim.** 2001. HIV-1 infection requires a functional integrase NLS. Mol. Cell **7:**1025–1035.
3. **Bukrinsky, M. I., and O. K. Haffar.** 1997. HIV-1 nuclear import: in search of a leader. Front. Biosci. **2:**d578–d587.
4. **Bukrinsky, M. I., S. Haggerty, M. P. Dempsey, N. Sharova, A. Adzhubel, L. Spitz, P. Lewis, D. Goldfarb, M. Emerman, and M. Stevenson.** 1993. A nuclear localization signal within HIV-1 matrix protein that governs infection of non-dividing cells. Nature **365:**666–669.
5. **Bukrinsky, M. I., N. Sharova, T. L. McDonald, T. Pushkarskaya, W. G. Tarpley, and M. Stevenson.** 1993. Association of integrase, matrix, and reverse transcriptase antigens of human immunodeficiency virus type 1 with viral nucleic acids following acute infection. Proc. Natl. Acad. Sci. USA **90:**6125–6129.
6. **Burke, C. J., G. Sanyal, M. W. Bruner, J. A. Ryan, R. L. LaFemina, H. L. Robbins, A. S. Zeft, C. R. Middaugh, and M. G. Cordingley.** 1992. Structural implications of spectroscopic characterization of a putative zinc finger peptide from HIV-1 integrase. J. Biol. Chem. **267:**9639–9644.
7. **Bushman, F. D., A. Engelman, I. Palmer, P. Wingfield, and R. Craigie.** 1993. Domains of the integrase protein of human immunodeficiency virus type 1 responsible for polynucleotidyl transfer and zinc binding. Proc. Natl. Acad. Sci. USA **90:**3428–3432.
8. **Cai, M., R. Zheng, M. Caffrey, R. Craigie, G. M. Clore, and A. M. Gronenborn.** 1997. Solution structure of the N-terminal zinc binding domain of HIV-1 integrase. Nat. Struct. Biol. **4:**567–577.
9. **Cannon, P. M., W. Wilson, E. Byles, S. M. Kingsman, and A. J. Kingsman.** 1994. Human immunodeficiency virus type 1 integrase: effect on viral replication of mutations at highly conserved residues. J. Virol. **68:**4768–4775.
10. **Charneau, P., and F. Clavel.** 1991. A single-stranded gap in human immunodeficiency virus unintegrated linear DNA defined by a central copy of the polypurine tract. J. Virol. **65:**2415–2421.
11. **Chen, J. C., J. Krucinski, L. J. Miercke, J. S. Finer-Moore, A. H. Tang, A. D. Leavitt, and R. M. Stroud.** 2000. Crystal structure of the HIV-1 integrase catalytic core and C-terminal domains: a model for viral DNA binding. Proc. Natl. Acad. Sci. USA **97:**8233–8238.
12. **Chow, S. A., K. A. Vincent, V. Ellison, and P. O. Brown.** 1992. Reversal of integration and DNA splicing mediated by integrase of human immunodeficiency virus. Science **255:**723–726.
13. **Cullen, B. R.** 2001. Journey to the center of the cell. Cell **105:**697–700.
14. **Depienne, C., A. Mousnier, H. Leh, E. Le Rouzic, D. Dormont, S. Benichou, and C. Dargemont.** 2001. Characterization of the nuclear import pathway for HIV-1 integrase. J. Biol. Chem. **276:**18102–18107.
15. **Devroe, E., A. Engelman, and P. A. Silver.** 2003. Intracellular transport of human immunodeficiency virus type 1 integrase. J. Cell Sci. **116:**4401–4408.
16. **Dirac, A. M., and J. Kjems.** 2001. Mapping DNA-binding sites of HIV-1 integrase by protein footprinting. Eur. J. Biochem. **268:**743–751.
17. **Dvorin, J. D., P. Bell, G. G. Maul, M. Yamashita, M. Emerman, and M. H. Malim.** 2002. Reassessment of the roles of integrase and the central DNA flap in human immunodeficiency virus type 1 nuclear import. J. Virol. **76:**12087–12096.
18. **Dyda, F., A. B. Hickman, T. M. Jenkins, A. Engelman, R. Craigie, and D. R. Davies.** 1994. Crystal structure of the catalytic domain of HIV-1 integrase: similarity to other polynucleotidyl transferases. Science **266:**1981–1986.
19. **Eijkelenboom, A. P., R. A. Lutzke, R. Boelens, R. H. Plasterk, R. Kaptein, and K. Hard.** 1995. The DNA-binding domain of HIV-1 integrase has an SH3-like fold. Nat. Struct. Biol. **2:**807–810.
20. **Engelman, A., and R. Craigie.** 1992. Identification of conserved amino acid residues critical for human immunodeficiency virus type 1 integrase function in vitro. J. Virol. **66:**6361–6369.
21. **Engelman, A., G. Englund, J. M. Orenstein, M. A. Martin, and R. Craigie.** 1995. Multiple effects of mutations in human immunodeficiency virus type 1 integrase on viral replication. J. Virol. **69:**2729–2736.
22. **Esposito, D., and R. Craigie.** 1998. Sequence specificity of viral end DNA binding by HIV-1 integrase reveals critical regions for protein-DNA interaction. EMBO J. **17:**5832–5843.
23. **Fassati, A., D. Gorlich, I. Harrison, L. Zaytseva, and J. M. Mingot.** 2003. Nuclear import of HIV-1 intracellular reverse transcription complexes is mediated by importin 7. EMBO J. **22:**3675–3685.
24. **Fouchier, R. A., B. E. Meyer, J. H. Simon, U. Fischer, A. V. Albright, F. Gonzalez-Scarano, and M. H. Malim.** 1998. Interaction of the human immunodeficiency virus type 1 Vpr protein with the nuclear pore complex. J. Virol. **72:**6004–6013.
25. **Freed, E. O., G. Englund, F. Maldarelli, and M. A. Martin.** 1997. Phosphorylation of residue 131 of HIV-1 matrix is not required for macrophage infection. Cell **88:**171–173.
26. **Gallay, P., T. Hope, D. Chin, and D. Trono.** 1997. HIV-1 infection of nondividing cells through the recognition of integrase by the importin/karyopherin pathway. Proc. Natl. Acad. Sci. USA **94:**9825–9830.
27. **Gallay, P., S. Swingler, J. Song, F. Bushman, and D. Trono.** 1995. HIV nuclear import is governed by the phosphotyrosine-mediated binding of matrix to the core domain of integrase. Cell **83:**569–576.
28. **Gerton, J. L., S. Ohgi, M. Olsen, J. DeRisi, and P. O. Brown.** 1998. Effects of mutations in residues near the active site of human immunodeficiency virus type 1 integrase on specific enzyme-substrate interactions. J. Virol. **72:**5046–5055.
29. **Goff, S. P.** 2001. Intracellular trafficking of retroviral genomes during the early phase of infection: viral exploitation of cellular pathways. J. Gene Med. **3:**517–528.
30. **Goldgur, Y., F. Dyda, A. B. Hickman, T. M. Jenkins, R. Craigie, and D. R. Davies.** 1998. Three new structures of the core domain of HIV-1 integrase: an active site that binds magnesium. Proc. Natl. Acad. Sci. USA **95:**9150–9154.
31. **Hansen, M. S., G. J. Smith III, T. Kafri, V. Molteni, J. S. Siegel, and F. D. Bushman.** 1999. Integration complexes derived from HIV vectors for rapid assays in vitro. Nat. Biotechnol. **17:**578–582.
32. **Heinzinger, N. K., M. I. Bukinsky, S. A. Haggerty, A. M. Ragland, V. Kewalramani, M. A. Lee, H. E. Gendelman, L. Ratner, M. Stevenson, and M. Emerman.** 1994. The Vpr protein of human immunodeficiency virus type 1 influences nuclear localization of viral nucleic acids in nondividing host cells. Proc. Natl. Acad. Sci. USA **91:**7311–7315.
33. **Heuer, T. S., and P. O. Brown.** 1997. Mapping features of HIV-1 integrase near selected sites on viral and target DNA molecules in an active enzyme-DNA complex by photo-cross-linking. Biochemistry **36:**10655–10665.
34. **Heuer, T. S., and P. O. Brown.** 1998. Photo-cross-linking studies suggest a model for the architecture of an active human immunodeficiency virus type 1 integrase-DNA complex. Biochemistry **37:**6667–6678.
35. **Hindmarsh, P., and J. Leis.** 1999. Retroviral DNA integration. Microbiol. Mol. Biol. Rev. **63:**836–843.
36. **Jenkins, T. M., D. Esposito, A. Engelman, and R. Craigie.** 1997. Critical contacts between HIV-1 integrase and viral DNA identified by structure-based analysis and photo-crosslinking. EMBO J. **16:**6849–6859.
37. **Jenkins, Y., M. McEntee, K. Weis, and W. C. Greene.** 1998. Characterization of HIV-1 vpr nuclear import: analysis of signals and pathways. J. Cell Biol. **143:**875–885.
38. **Katz, R. A., and A. M. Skalka.** 1994. The retroviral enzymes. Annu. Rev. Biochem. **63:**133–173.
39. **Katzman, M., and M. Sudol.** 1996. Influence of subterminal viral DNA nucleotides on differential susceptibility to cleavage by human immunodeficiency virus type 1 and visna virus integrases. J. Virol. **70:**9069–9073.
40. **Katzman, M., and M. Sudol.** 1998. Mapping viral DNA specificity to the central region of integrase by using functional human immunodeficiency virus type 1/visna virus chimeric proteins. J. Virol. **72:**1744–1753.
41. **Lewis, P., M. Hensel, and M. Emerman.** 1992. Human immunodeficiency virus infection of cells arrested in the cell cycle. EMBO J. **11:**3053–3058.
42. **Lewis, P. F., and M. Emerman.** 1994. Passage through mitosis is required for oncoretroviruses but not for the human immunodeficiency virus. J. Virol. **68:**510–516.
43. **Limon, A., E. Devroe, R. Lu, H. Z. Ghory, P. A. Silver, and A. Engelman.** 2002. Nuclear localization of human immunodeficiency virus type 1 preintegration complexes (PICs): V165A and R166A are pleiotropic integrase mutants primarily defective for integration, not PIC nuclear import. J. Virol. **76:**10598–10607.
44. **Limon, A., N. Nakajima, R. Lu, H. Z. Ghory, and A. Engelman.** 2002.

Wild-type levels of nuclear localization and human immunodeficiency virus type 1 replication in the absence of the central DNA flap. J. Virol. **76:**12078–12086.

45. **Lins, R. D., A. Adesokan, T. A. Soares, and J. M. Briggs.** 2000. Investigations on human immunodeficiency virus type 1 integrase/DNA binding interactions via molecular dynamics and electrostatics calculations. Pharmacol. Ther. **85:**123–131.
46. **Lodi, P. J., J. A. Ernst, J. Kuszewski, A. B. Hickman, A. Engelman, R. Craigie, G. M. Clore, and A. M. Gronenborn.** 1995. Solution structure of the DNA binding domain of HIV-1 integrase. Biochemistry **34:**9826–9833.
47. **Maertens, G., P. Cherepanov, W. Pluymers, K. Busschots, E. De Clercq, Z. Debyser, and Y. Engelborghs.** 2003. LEDGF/p75 is essential for nuclear and chromosomal targeting of HIV-1 integrase in human cells. J. Biol. Chem. **278:**33528–33539.
48. **Masuda, T., M. J. Kuroda, and S. Harada.** 1998. Specific and independent recognition of U3 and U5 att sites by human immunodeficiency virus type 1 integrase in vivo. J. Virol. **72:**8396–8402.
49. **Masuda, T., V. Planelles, P. Krogstad, and I. S. Chen.** 1995. Genetic analysis of human immunodeficiency virus type 1 integrase and the U3 att site: unusual phenotype of mutants in the zinc finger-like domain. J. Virol. **69:**6687–6696.
50. **Miller, M. D., C. M. Farnet, and F. D. Bushman.** 1997. Human immunodeficiency virus type 1 preintegration complexes: studies of organization and composition. J. Virol. **71:**5382–5390.
51. **Murakami, T., T. Hagiwara, K. Yamamoto, J. Hattori, M. Kasami, M. Utsumi, and T. Kaneda.** 2001. A novel method for detecting HIV-1 by non-radioactive in situ hybridization: application of a peptide nucleic acid probe and catalysed signal amplification. J. Pathol. **194:**130–135.
52. **Nakamura, T., T. Masuda, T. Goto, K. Sano, M. Nakai, and S. Harada.** 1997. Lack of infectivity of HIV-1 integrase zinc finger-like domain mutant with morphologically normal maturation. Biochem. Biophys. Res. Commun. **239:**715–722.
53. **Petit, C., O. Schwartz, and F. Mammano.** 2000. The karyophilic properties of human immunodeficiency virus type 1 integrase are not required for nuclear import of proviral DNA. J. Virol. **74:**7119–7126.
54. **Pluymers, W., P. Cherepanov, D. Schols, E. De Clercq, and Z. Debyser.** 1999. Nuclear localization of human immunodeficiency virus type 1 integrase expressed as a fusion protein with green fluorescent protein. Virology **258:**327–332.
55. **Reil, H., A. A. Bukovsky, H. R. Gelderblom, and H. G. Gottlinger.** 1998. Efficient HIV-1 replication can occur in the absence of the viral matrix protein. EMBO J. **17:**2699–2708.
56. **Roe, T., T. C. Reynolds, G. Yu, and P. O. Brown.** 1993. Integration of murine leukemia virus DNA depends on mitosis. EMBO J. **12:**2099–2108.
57. **Sayasith, K., G. Sauve, and J. Yelle.** 2000. Characterization of mutant HIV-1 integrase carrying amino acid changes in the catalytic domain. Mol. Cells **10:**525–532.
58. **Sherman, P. A., and J. A. Fyfe.** 1990. Human immunodeficiency virus integration protein expressed in Escherichia coli possesses selective DNA cleaving activity. Proc. Natl. Acad. Sci. USA **87:**5119–5123.
59. **Suzuki, Y., N. Misawa, C. Sato, H. Ebina, T. Masuda, N. Yamamoto, and Y. Koyanagi.** 2003. Quantitative analysis of human immunodeficiency virus type 1 DNA dynamics by real-time PCR: integration efficiency in stimulated and unstimulated peripheral blood mononuclear cells. Virus Genes **27:**177–188.
60. **Tsurutani, N., M. Kubo, Y. Maeda, T. Ohashi, N. Yamamoto, M. Kannagi, and T. Masuda.** 2000. Identification of critical amino acid residues in human immunodeficiency virus type 1 integrase required for efficient proviral DNA formation at steps prior to integration in dividing and nondividing cells. J. Virol. **74:**4795–4806.
61. **Vink, C., D. C. van Gent, Y. Elgersma, and R. H. Plasterk.** 1991. Human immunodeficiency virus integrase protein requires a subterminal position of its viral DNA recognition sequence for efficient cleavage. J. Virol. **65:**4636–4644.
62. **Vora, A., and D. P. Grandgenett.** 2001. DNase protection analysis of retrovirus integrase at the viral DNA ends for full-site integration in vitro. J. Virol. **75:**3556–3567.
63. **Wang, J. Y., H. Ling, W. Yang, and R. Craigie.** 2001. Structure of a two-domain fragment of HIV-1 integrase: implications for domain organization in the intact protein. EMBO J. **20:**7333–7343.
64. **Weinberg, J. B., T. J. Matthews, B. R. Cullen, and M. H. Malim.** 1991. Productive human immunodeficiency virus type 1 (HIV-1) infection of nonproliferating human monocytes. J. Exp Med. **174:**1477–1482.
65. **Wiskerchen, M., and M. A. Muesing.** 1995. Human immunodeficiency virus type 1 integrase: effects of mutations on viral ability to integrate, direct viral gene expression from unintegrated viral DNA templates, and sustain viral propagation in primary cells. J. Virol. **69:**376–386.
66. **Zack, J. A., S. J. Arrigo, S. R. Weitsman, A. S. Go, A. Haislip, and I. S. Chen.** 1990. HIV-1 entry into quiescent primary lymphocytes: molecular analysis reveals a labile, latent viral structure. Cell **61:**213–222.
67. **Zargarian, L., M. S. Benleumi, J. G. Renisio, H. Merad, R. G. Maroun, F. Wieber, O. Mauffret, H. Porumb, F. Troalen, and S. Fermandjian.** 2003. Strategy to discriminate between high and low affinity bindings of human immunodeficiency virus, type 1 integrase to viral DNA. J. Biol. Chem. **278:**19966–19973.
68. **Zennou, V., C. Petit, D. Guetard, U. Nerhbass, L. Montagnier, and P. Charneau.** 2000. HIV-1 genome nuclear import is mediated by a central DNA flap. Cell **101:**173–185.

Available online at www.sciencedirect.com
SCIENCE DIRECT®
Microbes and Infection 8 (2006) 670–679
Microbes and Infection
www.elsevier.com/locate/micinf

Original article

Human immunodeficiency virus type 1 Vpr induces cell cycle arrest at the G_1 phase and apoptosis via disruption of mitochondrial function in rodent cells

Akihiko Azuma [a], Ayako Matsuo [a], Tatsunori Suzuki [a,b], Terue Kurosawa [a], Xianfeng Zhang [a], Yoko Aida [a,b,*]

[a] *Retrovirus Research Unit, RIKEN, 2-1 Hirosawa, Wako, Saitama 351-0198, Japan*
[b] *Institute of Biological Science, University of Tsukuba, Tsukuba, Ibaraki 305-8572, Japan*

Received 5 April 2005; accepted 2 September 2005
Available online 11 January 2006

Abstract

Vpr of human immunodeficiency virus type 1 causes cell cycle arrest at the G_2/M phase and induces apoptosis after G_2/M arrest in primate cells. We have reported previously that Vpr also induces apoptosis independently of G_2/M arrest in human HeLa cells. By contrast, Vpr does not induce G_2/M arrest in rodent cells, but it retards cell growth. To clarify the relationship between cell cycle arrest and apoptosis, we expressed Vpr endogenously in rodent cells and investigated cell cycle profiles and apoptosis. We show here that Vpr induces cell cycle arrest at the G_1 phase and apoptosis in rodent cells. Vpr increased the activity of caspase-3 and caspase-9, but not of caspase-8. Moreover, Vpr-induced apoptosis could be inhibited by inhibitors of caspase-3 and caspase-9, but not by inhibitor of caspase-8. We also showed that Vpr induces the release of cytochrome *c* from mitochondria into the cytosol and disrupts the mitochondrial transmembrane potential. Finally, we showed that apoptosis occurred in HeLa cells through an identical pathway. These results suggest that disruption of mitochondrial functions by Vpr induces apoptosis via cell cycle arrest at G_1, but that apoptosis is independent of G_2/M arrest. Furthermore, it appears that Vpr acts species-specifically with respect to induction of cell cycle arrest but not of apoptosis.

Keywords: HIV-1Vpr; Apoptosis; Cell cycle arrest; Rodent cell; Mitochondrial function

1. Introduction

Vpr, one of the accessory proteins of human immunodeficiency virus type 1 (HIV-1), has many biological functions including nuclear translocation of the preintegration complex [1–5], induction of cell differentiation [6], regulation of apoptosis in both a positive and a negative manner [7–10], regulation of splicing [11], and cell cycle arrest at the G_2/M phase [12–16].

The induction of cell cycle arrest at G_2/M is particularly important, because the transcriptional activity of the HIV-1 long terminal repeat is most active at the G_2/M phase [17,18], and this activity leads to efficient virus production. It is not clear whether G_2/M arrest by Vpr is important in viral replication in vivo but such arrest of the cell cycle is a conserved feature of primate lentiviruses [19–22] and the open reading frame that encodes Vpr is maintained in vivo [18]. Thus, it seems likely that G_2/M arrest by Vpr might play an important role in the life cycle of HIV-1. Another important function of Vpr is the regulation of apoptosis. Significant levels of Vpr can be detected in the sera of AIDS patients [23] and Vpr is thought to play a role in the depletion of $CD4^+$ lymphocytes. Recent studies have provided evidence that apoptosis can occur either as a result of the expression

* Corresponding author. Retrovirus Research Unit, RIKEN, 2-1 Hirosawa, Wako, Saitama 351-0198, Japan. Tel.: +81 48 462 4408; fax: +81 48 462 4399.
E-mail address: aida@riken.jp (Y. Aida).

1286-4579/$ - see front matter © 2005 Elsevier SAS. All rights reserved.
doi:10.1016/j.micinf.2005.09.002

of Vpr endogenously or upon extracellular addition of Vpr to culture cells. Some studies have indicated that extracellular Vpr induces apoptosis via a direct effect on mitochondrial permeability [24,25]. Moreover, extracellular Vpr induces apoptosis in human neuronal cells through the activation of caspase-8 [26]. However, the mechanisms of apoptosis induced by the endogenous expression of Vpr remain to be clarified. The relationship between Vpr-induced cell cycle arrest and apoptosis remains largely unknown. It has been reported that Vpr-induced apoptosis occurs after G_2/M arrest [27]. By contrast, some authors have proposed that Vpr-induced apoptosis is independent of cell cycle arrest at the G_2/M phase [8,24,25]. In addition, Vpr of simian immunodeficiency virus, which infects African green monkeys, induces apoptosis in human cells but is unable to induce G_2/M arrest [28].

In a previous study, we reported that HIV-1 Vpr is able to interfere with the growth of mouse NIH3T3 fibroblastoid cells but failed to arrest these cells at the G_2 phase [29]. Our findings strongly suggest that Vpr might have another effect whereby it interferes with growth of the cells independently of G_2 arrest. Interestingly, we found that a carboxy-terminally truncated form of Vpr, C81, which failed to induce G_2/M arrest, retarded the growth even of human cells [30]. More recent studies showed that C81 induces apoptosis via G_1 cell cycle arrest in human cells [31] and this type of apoptosis is independent of G_2/M arrest [10]. Thus, it seemed possible that expression of Vpr in cells might cause apoptosis independently of the ability of Vpr to induce G_2 arrest. Indeed, we demonstrated that wild-type Vpr-induced apoptosis occurs by a mechanism that does not necessarily require induction of G_2 arrest in human cells [10]. In addition, replacement of Ile/Leu by Pro at positions 60, 67, 74, and 80 within the leusine zipper-like domain of wild type Vpr and C81 revealed that induction of apoptosis induced by Vpr and C81 processes might be regulated by the same pathway in human cells [10]. By contrast, we also showed that the activity of caspase-3 in extracts of C81-expressing cells is higher than that on extract of Vpr-expressing cells, suggesting that the induction of G_2/M arrest might inhibit the induction of apoptosis by Vpr in human cells [31]. We postulate that endogenous expression of Vpr might have a strong apoptotic effect in rodent cells, in which expression of Vpr does not induce G_2/M arrest. In fact, Yasuda et al. [32] reported that apoptosis occurs in transgenic mice that harbor the gene for HIV-1 Vpr. By contrast, there is also evidence to suggest that Vpr did not induce apoptosis in culture mouse cells in transient-transfection experiments [33]. Therefore, we decided to establish whether Vpr induces apoptosis in rodent cells and to investigate the detailed profile of cell cycle and the mechanism of Vpr-induced apoptosis in rodent cells.

In the present study, we transfected various lines of rodent cells and found that Vpr induced G_1 cell cycle arrest and apoptosis in all lines of rodent cells tested. Furthermore, we demonstrated that apoptosis occurred predominantly in Vpr-expressing cells. Moreover, Vpr induced apoptosis through the activation of caspase-3 and caspase-9 in rodent cells, with the associated release of cytochrome *c* from mitochondria into the cytosol and disruption of the mitochondrial transmembrane potential. Finally, we showed that Vpr induces apoptosis in human HeLa cells via an identical pathway. Our results suggest that disruption of mitochondrial function by Vpr induces apoptosis via G_1 cell cycle arrest and independently of G_2/M cell cycle arrest. Furthermore, we propose that Vpr acts species-specifically with respect to the induction of cell cycle arrest but not of apoptosis.

2. Materials and methods

2.1. Construction of plasmids

Generation of the expression vector pME18Neo, which encoded Flag-tagged wild-type Vpr, C81 and control Stop was described previously [10,11,29]. pEGFP-N1 encoded a "red-shifted" variant of wild-type green fluorescent protein (GFP) that had been modified for brighter fluorescence and has been used as a reporter molecule for discrimination between transfected and untransfected cells [34]. pSV-β-galactosidase encoded a bacterial β-galactosidase and was included for normalization of efficiencies of transfection.

2.2. Cell lines and transfections

Human cervical HeLa cells and baby hamster kidney fibroblasts BHK cells were maintained in RPMI 1640 medium supplemented with 3% heat-inactivated fetal calf serum (FCS), penicillin (100 U/ml), and streptomycin (100 μg/ml). Murine embryonic NIH3T3 cells and murine L fibroblasts (TK-) were maintained in medium supplemented with 10% FCS. Transfection of cells (1×10^7) was performed with the 25 μg or 50 μg of the indicated expression plasmid by electroporation with a Gene Pulsar (Bio-Rad, Richmond, CA).

2.3. Flow cytometry

All samples for flow cytometry were analyzed with a FACSort system (BD Immunocytometry Systems, San Jose, CA) with CellQuest software (BD Immunocytometry Systems). Relative numbers of cells in the G_1 phase, S phase and G_2/M phase were determined with ModFit LT software (Verity Software House, Topsham, ME).

The incorporation of BrdU was measured with a commercial BrdU Flow Kit (Becton Drive, Franklin Lakes, NJ) according to the manufacturer's instructions. In brief, 24 h after transfection, cells were incubated with 10 μM BrdU for 30 min and then harvested. Cells were then fixed, permeabilized, and treated with DNase for 60 min at 37 °C. Incorporated BrdU was detected with fluorescein isothionate-labeled (FITC-labeled) antibody against BrdU and Flag-tagged Vpr was detected with primary biotin-labeled Flag-specific antibody (Sigma, St, Louis, MO) and streptavidin-PE (BD Immunocytometry Systems) as secondary label.

For analysis of the cell cycle, cells were harvested and fixed with Cytofix/Perm buffer (Becton Drive). Then, they were incubated with biotin-labeled Flag-specific antibody for 30 min

on ice and then with streptavidin-FITC for 20 min on ice for detection of cells that expressed Vpr. DNA was stained with PI as described previously [10].

The active form of caspase-3 was detected with FITC-conjugated monoclonal active caspase-3 antibody apoptosis kit (Becton Drive) according to the manufacturer's instructions. Expression of Flag-tagged Vpr was detected as described above. DNA was stained with 7-aminoactinomycin D.

2.4. Western blotting

Twenty-four hours after transfection with 23.75 μg of a Vpr expression plasmid and 1.25 μg of pSV-β-galactosidase, cells were washed with phosphate-buffered saline (PBS) and divided into two aliquots: one aliquot was subjected to an assay of β-galactosidase activity (FluoReporter LacZ/Galactosidase Quantitation kit, Molecular probes, Eugene, OR) to monitor the efficiency of transfection and another aliquot of cells was lysed for 30 min on ice in 20 mM Tris–HCl (pH 8.0), 150 mM NaCl, 1% Nonidet P-40, 0.1% SDS supplemented with 0.2 mM sodium orthovanadate, 10 mM NaF, 10 mM β-glycerophosphate and a protease inhibitor cocktail (Roch, Indianapolis, IN). Lysates were centrifuged for 10 min at 15,000 × *g*, mixed with sample buffer for SDS-PAGE and then boiled for 5 min. Protein concentrations were determined with a BCA protein assay kit (Pierce, Rockford, IL) with BSA as the standard. Proteins in lysate with equal β-gal activity were examined by Western blotting as described previously [10]. Mouse monoclonal antibody against Rb (14001A) was obtained from BD PharMingen and used at a 1:1000 dilution. Mouse monoclonal antibody against Flag (M2) (Sigma) was used at a 1:2000 dilution. Mouse monoclonal antibody against cytochrome *c* (BioVision, Mountain View, CA) was used at a 1:200 dilution. Horseradish-peroxidase-conjugated sheep antibody against mouse IgGs was purchased from Amersham Bioscience (Uppsala, Sweden) and used at a 1:4000 dilution. Signals were visualized after treatment of the membrane with SuperSignal West Pico chemiluminescent substrate (Pierce).

2.5. Analysis of apoptosis

The activities of caspase-3, caspase-8 and caspase-9 were determined with a caspase-3/CPP32 fluorometric assay kit (BioVision), a caspase-8/FLICE fluorometric assay kit (BioVision) and a caspase-9/Mch6 fluorometric assay kit (BioVision), respectively, according to the manufacturer's protocol. In brief, 24 h after transfection, cells were harvested and lysed with cell lysis buffer. Each cell lysate was incubated with the appropriate substrate for 1 h at 37 °C. Measurement made with a multilabel counter (Model1420; Wallac Arvo; Perkin Elmer, Wellesley, MA). To analysis the effect of caspase inhibitors on Vpr-induced apoptosis, caspase-3/CPP32 inhibitor, Z-DEVD-FMK (BioVision), caspase-8/FLICE inhibitor, Z-IETD-FMK (BioVision) and caspase-9/Mch6 inhibitor, Z-LEHD-FMK (BioVision) were added to culture medium of transfected cells at final concentration of 2 μM. After 24 h, cells were harvested and apoptosis was determined by analysis of the activities of caspase-3, caspase-8 and caspase-9.

The release of cytochrome *c* was monitored with a cytochrome *c* releasing apoptosis assay kit (BioVision) according to the manufacturer's protocol. In brief, 24 h after transfection with 23.75 μg of a Vpr expression plasmid and 1.25 μg of pSV-β-galactosidase, cells were divided into two aliquots: one aliquot was subjected to an assay of β-galactosidase activity to monitor the efficiency of transfection and another aliquot of cells were homogenized with cytosol extraction buffer. The homogenate was centrifuged at 10,000 × *g* for 30 min and the supernatant was collected as the cytosolic fraction. Samples with equal β-gal activity were subjected to SDS-PAGE on a 15% polyacrylamide gel. Western blotting analysis was performed as described above.

The mitochondrial transmembrane potential was measured with a MitoCapture mitochondrial apoptosis detection kit (BioVision). In brief, 24 h after transfection, cells were washed with PBS and treated with trypsin. They were incubated with MitoCapture reagent at 37 °C for 15 min. Then samples were analyzed by flow cytometry. As a positive control, camptothecin was added to the growth medium at 1 μg/ml. Cells were harvested 12 h after the addition and analyzed by flow cytometry.

Hoechst 33258, which stains chromatin, was used to visualize the condensation and clumping of chromatin, as described elsewhere [35]. Thirty-six hours after transfection with 47.5 μg of a Vpr expression plasmid and 2.5 μg of pEGFP-N1, BHK cells growing on coverslips were fixed with 1% formaldehyde and then with 70% ethanol, and fixed cells were stained with Hoechst 33258 (Sigma, St. Louis, MO). Apoptotic bodies were characterized under fluorescence microscopy.

3. Results

3.1. Vpr induces cell cycle arrest at the G_1 phase in rodent cells

In various lines of primate cells, arrest of the cell cycle at G_2/M is induced by Vpr [12–16]. We reported that a carboxy-terminally truncated form of Vpr, C81, induces G_1 arrest but not G_2/M arrest in human HeLa cells [31]. However, Vpr failed to induce G_2/M arrest in mouse NIH3T3 cells [29]. In addition, the growth of NIH3T3 cells that stably expressed Vpr was suppressed [29]. To determine whether these observations depend on the species-specificity of the effect of Vpr, we examined the effects of Vpr on the growth of rodent cells.

We transfected BHK cells with plasmids that encoded Flag-tagged Vpr (Vpr) or Flag-tagged C81 (C81) or control vector Stop in which a Stop codon was inserted at the amino terminals of Vpr sequences. Cells were labeled with BrdU 24 h after transfection and BrdU incorporation was monitored by flow cytometry with FITC-conjugated antibody against BrdU. For identification of Vpr-expressing cells, cells were incubated with biotin-labeled Flag-specific antibody and then

with streptavidin-PE. As shown in Fig. 1A, cells transfected with Vpr and with C81 yielded 15.0 and 16.3% BrdU-positive cells, respectively. By contrast, BrdU-positive cells accounted for 30.9% of transfected with Stop. In particular, the majority of Vpr- and of C81-expressing cells were BrdU-negative (only 3.0 and 2.6% of cells were positive for incorporation of BrdU). Identical results were obtained 48 h after transfection in the case of the population of Vpr-expressing cells (data not shown). We concluded that the expression of Vpr or C81 caused the retardation of growth of BHK cells.

To determine whether growth retardation by Vpr occurred at a specific stage of the cell cycle, we analyzed the cell cycle distribution of BHK cells. Cells were stained with propidium iodide (PI) 24 h after transfection and analyzed by flow cytometry. About 13% of cells transfected with Vpr were in the S phase, compared with about 35% of the control cells (Stop). The number of Vpr-expressing cells at the G_1 phase was about 20% greater than that of control cells (Fig. 1B and Table 1). Identical results were obtained with C81-expressing BHK cells. Thus, the majority of Vpr-expressing BHK cells appeared to accumulate in the G_1 phase. To confirm this result, we performed a time course experiment (Table 1). Cells transfected with Vpr or C81 were arrested 24 h after transfection and G_1 arrest continued for at least another 24 h. However, we failed to observe an accumulation of cells in the G_1 phase after 72 h; we found only 5.7% and 1.1% of Vpr-expressing and C81-expressing cells, respectively (Table 1), and the majority of Vpr-expressing cells might have died.

Next, we prepared total cell extracts and examined Rb by Western blotting. Rb is progressively phosphorylated during the G_1 phase [36,37], and the phosphorylation status of Rb is thought to serve as a marker of cells in the G_0/G_1 phase

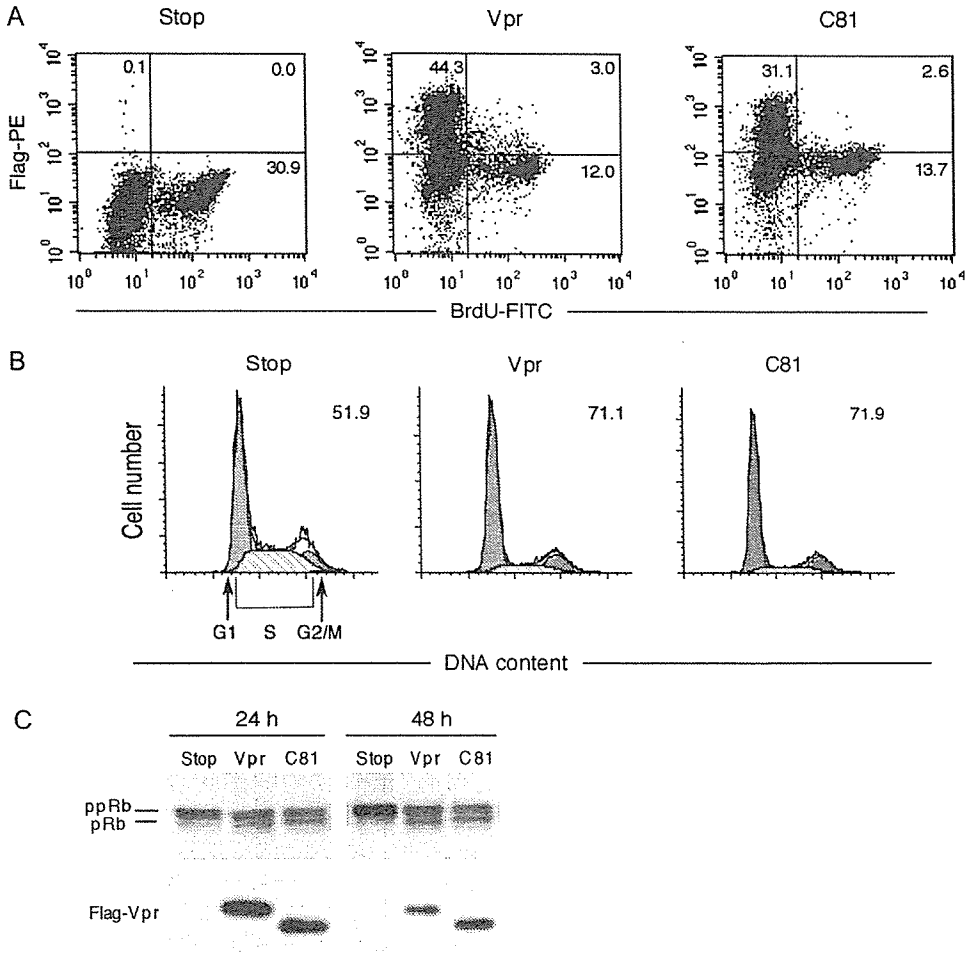

Fig. 1. Vpr induced G_1 cell cycle arrest in BHK cells. BHK cells were transfected with Stop, Vpr or C81 expression plasmids and then analyzed at indicated times. (A) BrdU incorporation was analyzed by flow cytometry. Twenty-four hours after transfection, cells were incubated with 10 μM BrdU for 30 min and then harvested. They were incubated with FITC-labeled BrdU-specific antibody and biotin-labeled Flag-specific antibody and then with streptavidin-PE for detection of cells that expressed Vpr. Samples were analyzed by flow cytometry. (B) Cell cycle profiles were analyzed by flow cytometry 24 h after transfection. Cells were incubated with biotin-labeled Flag-specific antibody and then with streptavidin-FITC for detection of cells that expressed Vpr. Then they were stained with PI for analysis of DNA content and analyzed by flow cytometry. Arrows indicate peaks of cell at the G_1 and G_2/M phase. The percent of cells at the G_1 phase is indicated at the upper right of each graph. (C) Cells were cotransfected with Stop, Vpr or C81 expression plasmids together with the β-galactosidase plasmid and cells were taken the measurements of β-galactosidase activity. Top photographs, lysates with equal β-galactosidase activity were examined for the phosphorylation of Rb by Western blotting. pRb, underphosphorylated Rb; ppRb, hyperphosphorylated pRb. Bottom, lysates with equal β-galactosidase activity were immunoblotted with Flag-specific antibody to monitor levels of expression of Vpr and C81.